Taphonomy of the Earliest Cambrian Linguliform Brachiopods

Authors: Forchielli, Angela, Steiner, Michael, Hu, Shixue, Lüter, Carsten, and Keupp, Helmut

Source: Acta Palaeontologica Polonica, 59(1) : 185-207

Published By: Institute of Paleobiology, Polish Academy of Sciences

URL: https://doi.org/10.4202/app.2011.0182

Taphonomy of the earliest Cambrian linguliform brachiopods

ANGELA FORCHIELLI, MICHAEL STEINER, SHIXUE HU, CARSTEN LÜTER, and HELMUT KEUPP

Forchielli, A., Steiner, M., Hu, S., Lüter, C., and Keupp, H. 2014. Taphonomy of the earliest Cambrian linguliform brachiopods. *Acta Palaeontologica Polonica* 59 (1): 185–207.

The Early Cambrian Burgess Shale-type fossil Lagerstätten of Yunnan Province (Chengjiang; Guanshan) are crucial in understanding the Cambrian bioradiation. Brachiopods are applied here as a critical model phylum to analyze the taphonomy of Yunnan fossil Lagerstätten, because shell and tissue composition of modern brachiopods can be compared with exceptionally preserved Cambrian remains. Systematic elemental mapping and energy-dispersive X-ray analyses have been carried out to study fossil brachiopods and their matrix from Cambrian Stages 3–4 and modern linguliform brachiopods from several geographical regions in order to evaluate the detailed structure of the shells and the biological and environmental influences on shell composition. Analyses of earliest Cambrian fossils encompassing the complete spectrum of weathering stages show a primary organo-phosphatic brachiopod shell, visible in unweathered specimens, and a successive dissolution and replacement of the shell during weathering, observable in specimens that underwent different stages of weathering. Therefore, our study reveals that earliest Cambrian linguliform brachiopods from the Chengjiang and Guanshan Biotas developed organo-phosphatic shells as their Recent counterparts. Early carbon and apatite preservation together with rapid deposition in claystone, instead of early iron adsorption, appears crucial for the preservation of highly delicate tissue. Primary calcium, phosphorus, organic carbon, and a multilayered shell are present, by inference between Cambrian fossils and Recent specimens, through the whole Phanerozoic. Elements such as silicon, sulphur, calcium, phosphorus, and iron were detected, impregnated with organic compounds in some organs of modern *Lingula*, and related to the potential of fossilization of Cambrian linguliform brachiopods. Ferromanganese precipitates traced in the shell of in vivo specimens of modern *Lingula* may enhance the potential for fossilization too.

Key words: Linguliformea, Brachiopoda, Chengjiang Fauna, Guanshan Fauna, taphonomy, elemental mapping, Cambrian, China.

Angela Forchielli [geoange@hotmail.it], Freie Universität Berlin, Malteserstraße 74-100, Haus D, 12249 Berlin, Germany, and Geological Survey of Austria, Neulinggasse 38, A-1030, Vienna Austria;
Michael Steiner [michael.steiner@fu-berlin.de], and Helmut Keupp [keupp@zedat.fu-berlin.de], Freie Universität Berlin, Malteserstraße 74-100, Haus D, 12249 Berlin, Germany;
Shixue Hu [hushixue@hotmail.com], Chengdu Institute of Geology and Mineral Resources, 610081 Chengdu, China;
Carsten Lüter [carsten.lueter@mfn-berlin.de], Museum für Naturkunde Leibniz-Institut für Evolutions- und Biodiversitätsforschung an der Humboldt-Universität zu Berlin, Invalidenstraße 43, 10115 Berlin, Germany.

Received 28 November 2011, accepted 25 April 2012, available online 4 May 2012.

Introduction

Study of the Chengjiang Fauna (Cambrian Stage 3, Yunnan Province, China) and Guanshan Fauna (Cambrian Stage 4, Yunnan Province, China) plays a pivotal role for understanding the Cambrian bioradiation. The preservational quality of the fauna led to numerous studies on topics such as taxonomy (e.g., Hou et al. 1988; Chen 2004; Luo et al. 2008), community structure (e.g., Zhao et al. 2009) and palaeoecology (e.g., Hu 2005; Hu et al. 2007b). However, the taphonomy of the Chengjiang Fauna and of the Guanshan Fauna is not yet well understood because a detailed study of the taphonomic pathways of these faunas based on unweathered or little weathered material is still lacking. Previous studies, which only were based on highly weathered material, define the Chengjiang fossil Lagerstätte as a Burgess Shale-type Lagerstätte, and suggest various taphonomic pathways involving the exceptional organic preservation of non-mineralizing organisms, such as organic film preservation (Butterfield 1995, 2002, and 2003) or pyritization (subsequently replaced by iron oxide pseudomorps after pyrite; Gabbott et al. 2004).

The Chengjiang-type Fauna of Yunnan has been intensively studied because it contains remarkably high biotic diversity. In the last 10 years, the stratigraphically younger Guan-

http://dx.doi.org/10.4202/app.2011.0182

shan Fauna has also received increasing attention, as it also possesses a high faunal diversity and highly delicate tissue structures (Luo et al. 1999, 2005, 2007; Hu et al. 2007a, 2008, 2010a, b). Almost all metazoan clades occurring in the Chengjiang Fauna are present in the Guanshan Fauna, including trilobites, bradoriids, vetulicolids, priapuliids, brachiopods, anomalocaridids, chancelloriids, sponges, hyolithids, algae, and trace fossils (Luo et al. 2008). The Chengjiang-type Fauna encompasses more than 120 genera (or 150 genera as suggested by Zhang et al. 2008a) with 140 species belonging to 24 phyla (Han et al. 2006 and references therein). The Guanshan Fauna was described from the Kunming District (Yunnan Province, China; Luo et al. 1999, 2005, 2006, 2007, 2008; Hu et al. 2007a, 2010b) and it currently comprises about 60 taxa belonging to 10 different fossil groups (Hu et al. 2010b).

Brachiopods represent 24% of the individuals of the Chengjiang Fauna in the event beds (EB) and 0.7% in the background beds (BGB) in a section near Haikou, Kunming (Zhao et al. 2009) and are the second most important metazoan group after arthropods in terms of abundance and diversity in the Guanshan Biota (Hu et al. 2010b). Because brachiopods are widely found in the earliest Cambrian Burgess Shale-type fossil Lagerstätten in Yunnan Province, we propose to use them as a critical model phylum for taphonomic analyses, allowing comparison with modern material. Living specimens are used to show what kinds of patterns are expected in fossil material. Fossil specimens are used to test the hypothesis that the construction of the shell material of linguliform brachiopods has remained constant through the history of this clade. In addition, their highly delicate tissues are often preserved, including lophophore, pedicle, setae, and more rarely the mantle canal, digestive tract, and visceral region. Soft-tissue preservation is important because it enables comparison between fossil and extant bauplans of linguliform brachiopods. Two different types of tissues are examinated in fossil material: shell material, which may contain an organic matrix (that can be subsequently lost to diagenesis) and soft tissues.

Previous work on the Cambrian brachiopod assemblage from the eastern Yunnan comprises eleven reported genera, of which one is assigned to the Subphylum Rhynchonelliformea, and the other ten to the Subphylum Linguliformea, (Zhang et al. 2008b). Among the Chengjiang linguliform brachiopods, *Lingulellotreta malongensis* Rong, 1974 and the obolid *Lingulella chengjiangensis* Jin, Hou, and Wang, 1993 are numerically dominant (Jin et al. 1993; Zhang et al. 2007). In the Guanshan Biota, *Lingulellotreta malongensis*, *Diandongia pista* Rong, 1974, and *Heliomedusa minuta* Luo and Hu, 2008 are dominant (Hu et al. 2010b).

Palaeozoic linguliform brachiopods were presumed to have developed organo-phosphatic shells, but, owing to the variety of pristine Palaeozoic fossil material and the uncertain influence of diagenetic phosphatization, the detailed primary shell construction in earliest Cambrian linguliform brachiopods remained an open question for a long time. In this study primary shell construction of linguliform brachiopods from the Chengjiang Fauna, the Guanshan Fauna and from the Sinsk Biota (Botoman Stage, Siberia, Russia) is analyzed and compared with the shell construction of the Recent genera *Lingula* Bruguière, 1797 and *Glottidia* Dall, 1870 from Japan, China, Thailand, Australia, and California. In addition, confusion on this topic has been generated by authors who refer to the shells of linguliform brachiopods as phosphatic instead of organo-phosphatic (Bengston 2005: 105). Most of the previously studied organo-phosphatic shelled brachiopod material presents not a pristine signal but a solid, compact phosphatic shell that did not retain organic material or primary structures such as tubules. These structures have been well described by Iwata (1981). The tubules are not mineralized and develop nearly perpendicular to the inner surface of the shell. They penetrate the mineralized layer and become slender in the organic layer. They thin out in the middle part of the organic layer (Iwata 1981). Therefore, it appeared relevant to evaluate whether early Cambrian brachiopod shells represent primary biominerals or diagenetic replacements. Small shelly fossils (SSFs) represent an informal group of small (mostly millimetric), primarily or secondarily mineralized (phosphatized, silicified, carbonatic, limonitic) remains (skeletal and non-skeletal) of metazoans which have a world-wide occurrence at the Precambrian–Cambrian boundary. The occurrences of large numbers of phosphatic SSFs led some authors (e.g., Lowenstam 1981) to the assumption that phosphate was the dominant primary biomineral for the formation of skeletons in most metazoan clades during the Cambrian period. Most phosphatic SSFs are now considered to be the result of early or later phosphate permineralization, coating, and replacement (Steiner 2008; Forchielli et al. 2009; Steiner et al. 2010). The remaining candidates for primary phosphate biomineralization are mobergellids, tommotids, tannuolids, the *Hyolithellus* group, palaeoscolecids sensu stricto, tubular remains of *Byronia* and *Sphenothallus*, Phosphatocopina, conulariids, and linguliform brachiopods. This study aims to use the two extant genera of organophosphatic-shelled linguliform brachiopods, *Lingula* Bruguière, 1797 and *Glottidia* Dall, 1870, as a key to understanding the fossilization potential of the different organs and the taphonomic pathways of the earliest Cambrian linguliform brachiopods, and to examine how the environment might have influenced the shell minerals and structure of living linguliform brachiopods.

Institutional abbreviations.—AF, FU, MS, Freie Universität Berlin, Germany; GKG, Maf, Yunnan Institute of Geological Sciences, Kunming, China; GZG, Geoscience centre of the University of Göttingen, Germany; TU, Technische Universität Berlin, Germany; UCL, University College London, UK; ZELMI, Zentraleinrichtung Elektronenmikroskopie, Berlin, Germany; ZMB, Museum für Naturkunde Leibniz-Institut für Evolutions- und Biodiversitätsforschung an der Humboldt-Universität zu Berlin, Germany.

Other abbreviations.—BGB, background beds; BSD, backscattered detector; CT, computer tomography; EB, event beds;

EDX, energy-dispersive X-ray; GAGs, glycosaminoglycans; ICP, digestion-inductively coupled plasma; TOC, total organic carbon; SSFs, small shelly fossils; WDS, wavelength dispersive spectrometer.

Material and methods

Fossil material from the Cambrian described here was collected from the Xiaolantian, Xiaotan, Shitangshan, and Haikou-Chengjiang sections of Yunnan Province. It was recovered from the Yu'anshan Formation (Chengjiang Fauna) and the Wulongqing Formation (Guanshan Fauna). The Canglangpuan sediments yielding the Guanshan Fauna (northwest of Kunming, Yunnan Province) were deposited as event beds in relatively shallow water environments (Luo et al. 2008; Hu et al. 2010b). The deposition environment of the Wulongqing Formation (Canglangpuan Regional Stage, Cambrian Series 2) is interpreted as offshore transition (Hu et al. 2010b). Soft-bodied fossils-containing layers generally show graded silt-muds couplets with erosive bases, indicating rapid setting from distal storm. Sedimentological and taphonomic analyses indicate that the unusual preservation of the soft-bodied fossils is resulted from the smothering of storm induced rapid burial. The Chengjiang fossil Lagerstätte (Cambrian Stage 3) is characterized by couplets of BGBs and EBs. BGBs are mostly absent in the fossil Lagerstätte of the Guanshan, probably due to extremely rapid deposition and partial sediment reworking in a shallow-water setting.

Linguliform brachiopod shells from SSF samples were collected from the Lower Yu'anshan Formation in the Xiaotan section (Yongshan County, China).

The material from the Sinsk Biota comes from the Ulakhan-Touydakh section at Lena River (Siberia, Russia) and was collected during the XIII International Field Conference of the Cambrian Stage Subdivision Working Group, Yakutia 2008. The brownish, thin-plated silty carbonates of the Sinsk Formation (Botoman Regional Stage) yielding this fauna contained the genus *Eoobolus* Matthew, 1902. The Sinsk biota inhabited an open-marine basin within the photic zone, but in oxygen-depleted bottom waters (Ivantsov et al. 2005). Rapid burial in a fine-grained sediment under anoxic conditions contributed to Burgess Shale-type preservation in one of the earliest Russian Cambrian fossil Lagerstätten (Ivantsov et al. 2005; Hu et al. 2010b; Ponomarenko 2010).

The studied Recent specimens of *Lingula anatina* are from Japan (Kasari Bay, Amami Island and Ariake Bay, Kyushu), Guangdong Province, China (intertidal sand of the South China Sea), Thailand (Rayong Province, Gulf of Thailand), and Australia (Stradbroke Island, Queensland housed at GZG and Magnetic Island, Queensland); *Lingula adamsi* comes from Guangxi Province, China (subtidal black sandy mud of the Beibu Gulf); one specimen of *Glottidia albida* is from California, and several specimens of *Glottidia palmeri* are from the northeastern Baja California, Mexico (intertidal silty clays of Vega Island). The studied larva of *L. anatina* with 9 paired cirri (9 p.c.) was collected from a plankton haul, off Magnetic Island, Queensland, Australia and was pre-fixed with 2.5% glutardialdehyde, buffered with sodium cacodylate and postfixed in aequeous solution of OsO_4 1% for 40 minutes. Analyses of the specimens from Kasari Bay, Amami Island, Japan strongly suggest that this population represents an undescribed sibling species different from *L. anatina* (Nishizawa et al. 2010). The genus *Glottidia* differs from the genus *Lingula* by the presence of septa in the internal valve faces and papillae in the mantle and by the baculation of its shell, absent in *Lingula*, but present in *Discinisca* (Iwata 1981, 1982) and also found in shells of Early Palaeozoic linguliform brachiopods (Holmer 1989).

Elemental mapping was performed using two energy-dispersive X-ray (EDX) analysers: a Kevex delta V energy-dispersive elemental analyser with a quantex light element detector coupled to a S-2700 SEM HITACHI and an Inca analyser X-max 50 mm^2 coupled to a SEM ZEISS-SUPRA 40VP; uncoated and unpolished fossils were analysed using 20 kV, 15 kV, and 10 kV. For this study we analyzed fossil linguliform brachiopods embracing the complete spectrum of weathering stages, from unweathered to weathered grades. Recent specimens were prepared with a four component resin (Epon 812) suitable for SEM analyses before cutting. Specimens were analyzed after polishing and carbon-coating using 20 kV, 15 kV, and 10 kV. Apatite of a modern *L. anatina* from Japan was analyzed with a Cameca Cameback Microbeam Microprobe to discern the nature of the apatite of the shell. A section of the shell valve was line scanned (5 seconds per count) with a wavelength dispersive spectrometer (WDS) detector below the median adductor muscle and element peaks plotted after background was subtracted. Specimens of *L. anatina* and *Glottidia palmeri* with labile tissues preserved in ethanol were prepared with a CPD 030 Critical Point Dryer (BAL-TEC) and then analyzed with a nanofocus-X-ray computed tomograph Phoenix Nanotom 180 kV. Once scanned, the fully three-dimensional CT information allows non-destructive visualization of slices or arbitrary sectional views. Since the whole geometry of the object is scanned, precise 3D measurements of complex objects are possible. We use this method to analyze spatial distribution of the internal organs of the specimens. SSF extraction from carbonate samples followed standard techniques using 10% acetic acid. Some of the fossils used for SEM investigation were mounted on stubs using double-sided adhesive carbon tape and covered with gold; the rest of the fossils were prepared with a bicomponent resin (Araldit 2020) suitable for SEM analyses, and the layered structure of their shells was analyzed in cross section. Histological sections were used to identify the different organic components/tissues of the internal organs using longitudinal serial sections of a whole subadult specimen from Magnetic Island, Australia fixed in Bouin's fluid. The organo-phosphatic shell was softened using diaphanol (3 days, room temperature). After dehydration through an alcohol series, butanol and methyl benzoate, the specimen was embedded in paraffin and subsequently sectioned (10 μm) with a Reichert Histo-

http://dx.doi.org/10.4202/app.2011.0182

Microtome. Serial sections were mounted on glass slides and stained with the Azan method (after Geidies 1954). Geochemical analyses were done at Actlabs (Activation Laboratories Ltd.), Canada (main and trace elements) using 4 acid digestion-inductively coupled plasma (ICP), instrumental neutron activation analysis (INAA) and lithium metaborate/ tetraborate fusion ICP; samples were analysed for nitrogen, sulphur, and total carbon (TC) by a CNS-Analyser (Elementar Vario EL III) and for total organic carbon using an Elementar Vario Max at AWI Potsdam and an Elementar LiquiTOC at TU Berlin; iron speciation was performed at New Castle University, according to Poulton and Canfield's (Poulton et al. 2004; Poulton and Canfield 2005) sequential extraction procedure for iron.

Results

Shell.—The linguliform brachiopods from the Guanshan Fauna, like those from the Chengjiang Fauna, occur as flat impressions in an alumino-silicate clay matrix. BSD and EDX analyses of shell remains of *Lingulellotreta* from least weathered strata of the Burgess Shale-type fossil Lagerstätte of Guanshan show couplets of alternating apatite and organic layers (revealed by EDX analyses). Pores and tubules are visible in the whole shell (Fig. 1A, B, E). This type of layered shell with preserved tubules is interpreted here as the primary shell structure without diagenetically overgrown apatite. However, this preservation is also rare in the Guanshan fossil Lagerstätte. Most fossil shell remains show massive apatitic layers with no preserved pores or tubules, even if the bed yielded exceptionally well preserved fossils with detailed micro-structures.

Juvenile shells of brachiopods recovered with other SSFs from the Yu'anshan Formation of the Xiaotan section, which is well known for its Orsten-type preservation (e.g., Zhang 2007), also revealed multilayered shells (Fig. 1D) interpreted here as primary shell that is diagenetically partially altered.

The isolated shells of *Eoobolus* from the Sinsk Biota show (Fig. 1F, H) a layered construction, too. In the transversal section (Fig. $1H_1$), which probably represents the marginal part of the shell (compare Fig. $2C_2$ for the modern *Lingula*), five to six couplets of compact and porous layers are visible. In the longitudinal section (Fig. $1F_1$) sub-parallel layers are preserved. The disposition of the layers is similar to those of the extant representatives in the median region of longitudinal shell sections (Fig. 3E–H). Here compact layers and more porous layers exist, separated from each other probably during sample grinding. The colour difference visible in the BSD is probably due to incorporation of some lighter elements, such as organic compounds, in the mostly apatitic shell. Furthermore, a net-like structure is present in the porous layer.

Detailed comparison of fossil linguliform brachiopods *Lingulella* and *Lingulellotreta* and modern *Lingula* reveals a similar sandwiched composition of thin apatitic interlayers with tubules in an organic shell matrix (Fig. 1G). Elemental mapping and EDX analyses of various Recent species of *Lingula* from different geographical regions (e.g., *Lingula anatina* from Japan, China, Thailand, and Australia) show no significant variation in shell composition and structure within the species due to geographical and environmental factors. The number of phosphatic layers within the shell, for the same species, shows no geographical variation. On the contrary, a variation in the number of phosphatic layers is evident among specimens of modern linguliform brachiopods among different genera (e.g., *Lingula* and *Glottidia*) and also among different species of the same genus (e.g., *L. anatina* and *L. adamsi*). In shells of *Glottidia,* apatite is not only present in the biomineralized layers but also in the organic ones, where the organic fibres, impregnated with apatite crystallites, are arranged in a net (Fig. 4; see also Holmer 1989: fig. 21), so that *Glottidia* has a higher apatite content than *Lingula*, even if *L. anatina* has usually more biomineralized layers than *Glottidia*. Previous studies performed using solid-state nuclear magnetic resonance (SSNMR) spectroscopy (Neary et al. 2011) also confirmed that *Lingula* and *Glottidia* have different spectra except for the chitin components, and most of these differences are related to protein signals, demonstrating the different amino acid composition of the two shells (Jope 1969; Williams et al. 1998). The greatest number of phosphatic layers is always present below the median adductors in all investigated species, while they decrease towards the apical and posterior ends of the shell. *L. anatina* has an usually large number (10–15) of apatite layers (counted below the median adductors), whereas *L. adamsi* possesses only three layers (Fig. 5) and a thick undulate structure containing different mineral components underneath an outer periostracum (Fig. 1C) similar to that reported by Williams et al. (1998 and 2001) for *Discinisca*, which shows folds in the primary layer. Semi-quantitative EDX

Fig. 1. Shell structures of linguliform brachiopods. **A**. *Lingulellotreta* (AF Shit4 088a) from Guanshan Fauna, Cambrian (Gaoloufang section, Kunming); layered shell structures are visible in unweathered specimen; detail of the layered shell structure (A_1), longitudinal sections (A_2), and whole specimen (A_3). **B**. *Lingulellotreta* (MS-WLG1) from Guanshan Fauna, Cambrian (Gaoloufang section, Kunming), an organic carbon layer with pores is visible under the apatite layer; whole specimen (B_1), detail of B_1 (B_2). **C**. Recent specimen of *Lingula adamsi* Dall, 1873 (MS-Ch.L.ad) from China; an undulate structure visible in the external part of the shell (C_1), white material in the most external part is rich in Si, whereas the white layer in the inner part is apatite; detail of C_1 (C_2), detail of C_2 (C_3). **D**. *Lingulella* (MS-XTN6-AF) from the Xiaotan section, Cambrian, layered structure preserved (D_1) and overview of the specimen (D_2). **E**. *Lingulellotreta* (AF Shi 4-0818) from Guanshan Fauna, Cambrian (Shitangshan); tubules visible on the surface of one of the layers (E_1, arrowed); layered shell (E_2). **F**. *Eoobolus* (MS-UTS-Si-001) from Sinsk Biota, Cambrian (Siberia); whole specimen (F_2), longitudinal section (F_1). **G**. Recent *Lingula anatina* Lamark, 1801 (ZMB Bra 1861); layered shell in light microscope (G_1) and SEM (G_2) images. Arrows point out the tubules. **H**. *Eoobolus* (MS-UTS-Si-002) from Sinsk Biota, Cambrian (Siberia); transversal section (H_1), detail of H_1 (H_2). Compact and porous couplets are well visible in both sections. →

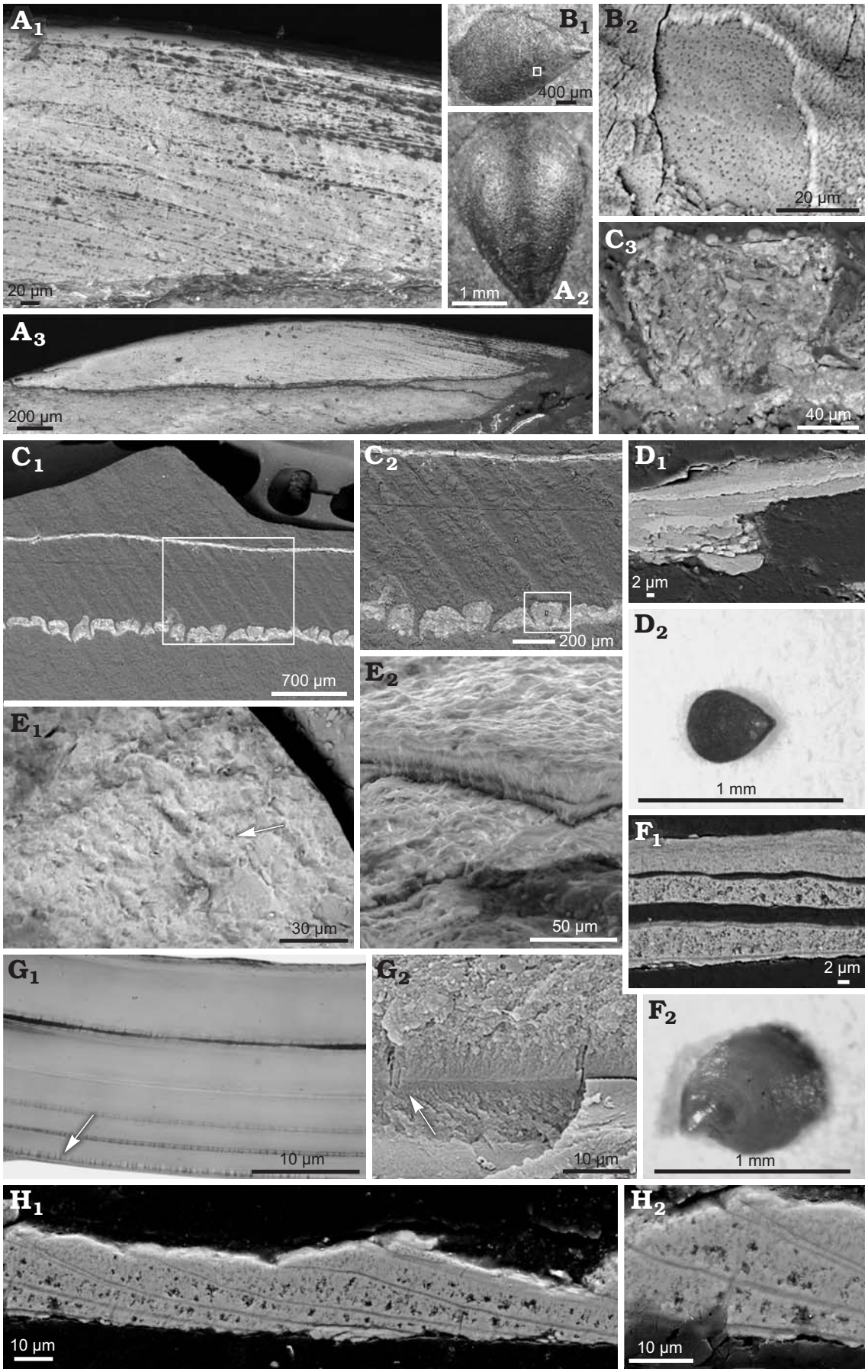

http://dx.doi.org/10.4202/app.2011.0182

analyses of the undulated layer show enrichments of silicon (Fig. 6C), aluminum (Fig. 6D), carbon, oxygen, manganese (Fig. 6E), and iron (Fig. 6F) in this layer that form thicker mineralized pockets between concentric ridges (see frame in Fig. 1C). Si occurs in platy structures (about 11 μm in length; Fig. 6A: red dot, B) that show similarities with the siliceous tablets of the larval shell of *Discinisca* (Williams et al. 1998). Al and Si co-occur within granular structures that may represent aluminosilicates (Fig. 6C, D). Nodular structures are present within the outer mineralized layer (about 8 μm in diameter). These are enriched in Mn and Fe (Fig. 6A, G) and extend into the organic shell layer. The ferromanganese precipitate reveal a concentric growth structure with incorporation of apatite, carbon, and Mn-, Fe-oxides (?hydroxides) (Fig. 6G and point analyses 1, 2, and 3). The growth centre of the ferromanganese precipitate are mostly enriched in Fe relative to the outer part and the nodules radiate from a clearly defined lamina between the mineralized outer layer and the unmineralized shell into the organic shell. Fe is also enriched in the outer part of periostracum as in *L. anatina* (Fig. 6F).

Study of shell mineralogy and structure was first undertaken by Blochmann (1900) at the beginning of the last century. Understanding was improved considerably by two contributions from Iwata (1981, 1982) who identified shell minerals similar to francolite, and by the study of Williams et al. (1994). The primary shell layer is defined as mineralized and 30–50 μm thick (Emig 1990), and mostly consists of the organic compounds glycosaminoglycans (GAGs; Cusack et al. 1999). Our analyses support the previous observation that the primary shell layer is made of organic matter about 20 μm thick. Volume percent calculation of different shell constituents along longitudinal sections of *Glottidia albida*, *L. anatina*, and *L. adamsi* show only slight variation in the volume percentages of apatite (V_{ap}%) and organic matter (V_c%) for *Glottidia albida* (V_{ap}% varies between 29.6% and 53.9%; V_c% varies between 46.1 % and 70.4%). However, there is considerable variability in volume constituents in individual shells and between different species of the genus *Lingula*. For *L. anatina* V_{ap}% varies between 5.4% (at the anterior end) and 50.4% (below the median adductors), whereas for *L. adamsi* it varies between 3.9% and 14.2%. The V_c% ranges between 49.6% and 94.6% for *L. anatina* and between 85.7% and 96.1% for *L. adamsi*. Under the theoretical assumption of the density of apatite (3.2 g/cm^3) and that of organic matter (1.4 g/cm^3) and a 30% penetration of apatite in the organic layers for *Glottidia albida*, the shell composition expressed in weight percent (Wt%) of apatite reaches a maximum of 66% for *Glottidia albida*, 27.7% for *L. adamsi*, and 70% for *L. anatina*. Observations based on our specimens confirm the assumption made by Iwata (1981) that apex and shell margin of the *Lingula* shell were not mineralized, and show that shell growth of the species *L. anatina* and *L. adamsi* is by secretion from the mantle at the lateral and anterior shell region. Phosphate deposition does not immediately co-occur with new shell secretion. Thus phosphatic layers only occur 900 μm from the anterior end of the shell and about 400 μm from the lateral shell margin. Analyses of the larva of *L. anatina* also reveal that the larval shell, about 7–8.5 μm thick, does not contain any lamellae: it is a uniform organic layer (Fig. 7A, G). There are no element enrichments other than Os and P, representing artefacts of fixation, in the soft tissue or shell of studied *Lingula* larva and Ca occurs only in small granules, maybe also due to fixation artifacts (Fig. 7D–F). The Fe-enrichment often detected in the periostracum of mature shells could not be found in the larva (Fig. 7C). The investigated larval shell (Fig. 7G) is 7.6 μm thick and the outer 0.5 μm of shell are stained by Os due to the fixation. Underneath the shell is another electron-denser layer 1.8 μm thick (Fig. 7F, G) representing mantle tissue stained with OsO_4. There is no Fe enrichment or Si in the internal organs as for the adults *Lingula*. It can be assumed that phosphate formation occurs in a later ontogenetic stage than the investigated 9 paired cirri larva.

WDS microprobe analyses of *L. anatina* show a fluorapatite composition of the shell with fluorine values between the 2.6 Wt% of the external layer (Figs. 8, 9A) and 3.5 Wt% of the internal layer (Figs. 8, 9C); magnesium (Mg) is present, with Wt% of 1.5 for the external layer, 2.9 for the median part of the shell and 2.4 for the internal layer, and traces of sodium (Na), and sulphur (S) are visible from the EDS analyses (Fig. 9).

Soft tissues in fossil material.—Detailed reviews given by Zhang et al. (2004a, b, 2005, 2007, 2008b) and by Zhang et al. (2003a) for Chengjiang linguliform brachiopods from the Ercaicun site (Yunnan Province) show the presence of soft-tissues in 9.8% (1000 counts) and 12% (400 counts) of individuals respectively. Our data show similar values of 11.8% (n = 127) for soft part preservation of brachiopods in the Chengjiang-type fossil Lagerstätten of Yunnan. Lophophore (Fig. 10B, C, E) and pedicles (Fig. 10A, D, E) are the most commonly preserved soft parts. Preliminary results for Guanshan Fauna given by Hu et al. (2010a) are concordant: among 20 individuals, 12 show preserved pedicles and 2 show lophophores. As observed in CT analyses of our specimens and confirmed by histological sections, the pedicle

Fig. 2. Diverse analysis methods applied to shells of Recent *Lingula anatina* Lamark, 1801. **A**. Histological section of a sub-adult specimen (ZMB Bra 2241) from Australia. Enlargement of the lophophore (A_1), connective tissue in blue, muscles in orange to brown, nuclei in red, and grayish colours represent parts of the nerve system; detail of A_1 (A_2). Enlargements of the digestive glands (A_3) and of the meta-nephridium and part of the gut (A_4); detail of A_4 (A_6), the gray dots in the gut are mucus transporting newly captured food to the digestive glands and at the same time collecting remains of the diet (e.g., broken diatom shells etc.). Enlargement of the pedicle, which is visibly connected with the coelom (A_5). **B**. Transversal section from a Nano CT-X-ray analysis focused on lophophore (AF CPD JEn.An) from Japan. Lophophore (B_2), the arrow points to the mouth; the maximal longitudinal length is 9.35 mm. Longitudinal view of the U-shaped gut (arrow) and pedicle (B_1); the scale bar on B_1 applies only to the x-y dimension of this 3D reconstruction. **C**. Elemental mapping of (AF JL.An.Tra) from Japan. The metanephridium (C_1); external layer in the marginal area of a transverse section (C_2). Blue shows the Fe (K alpha). →

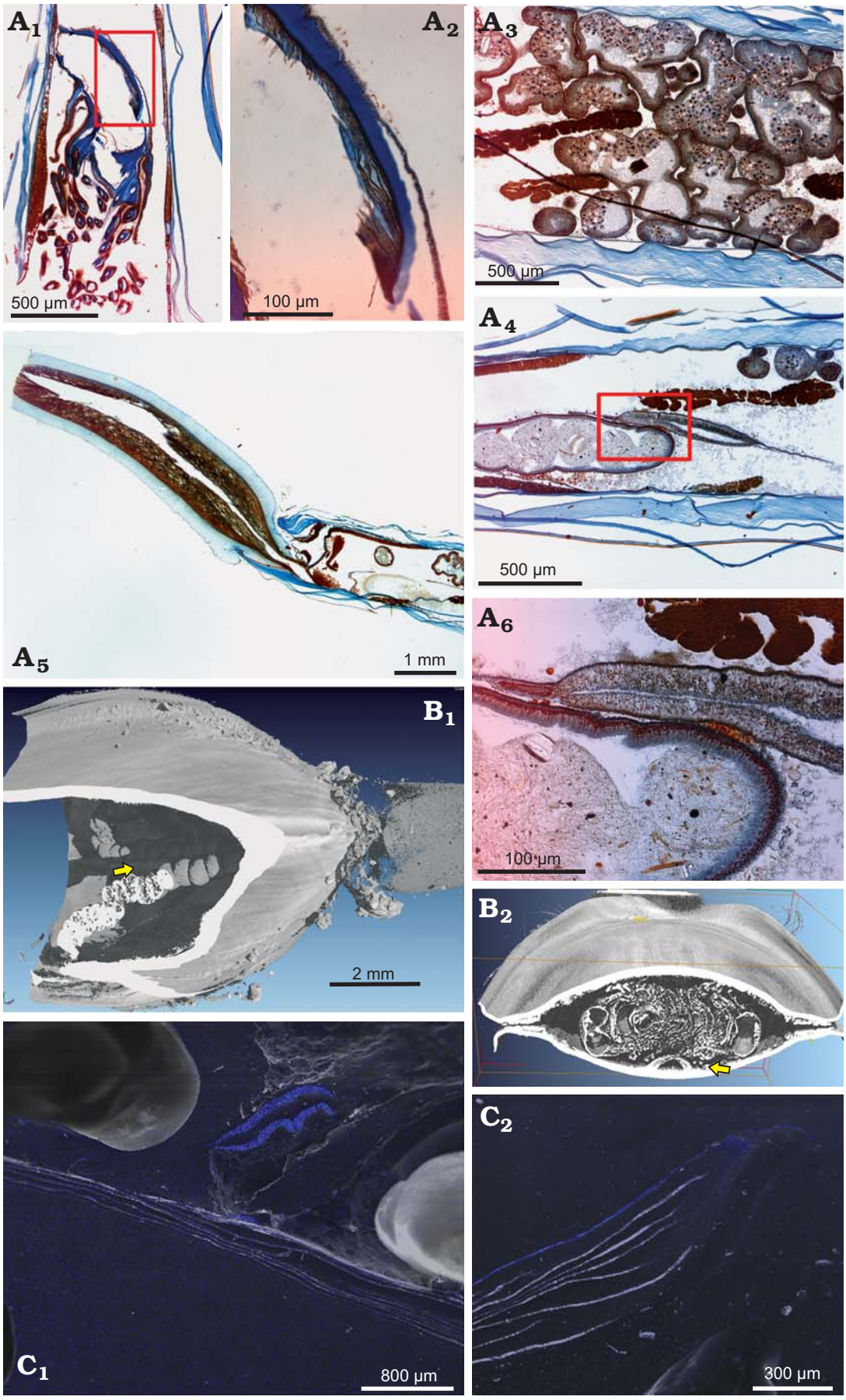

http://dx.doi.org/10.4202/app.2011.0182

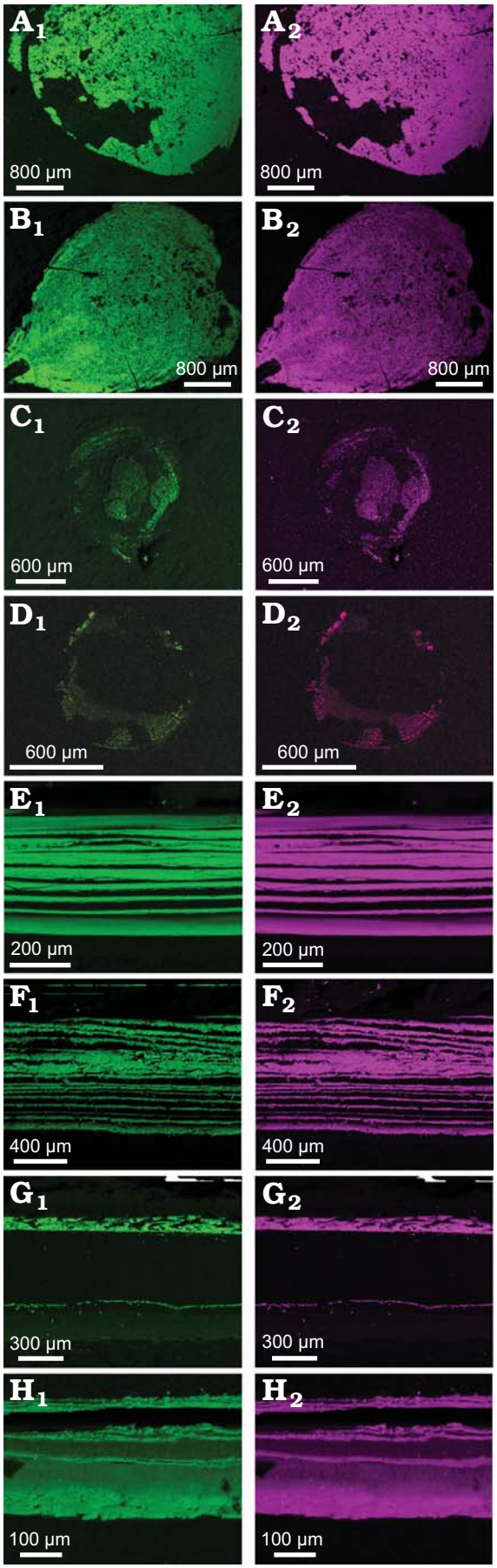

coelom is connected to the mantle coelom during life in *Lingula*. In fossil specimens the coelom is visible—and in very rare cases preserved–as a darker midline through the length of the fossilized pedicle (Fig. 10A, D, E). The lophophore revealed an iron composition in all brachiopod specimens analyzed from the Chengjiang-type Fossil Lagerstätten of the Yunnan province, (e.g., *Lingulella*, *Lingulellotreta*, *Diandongia*, and *Heliomedusa*) without showing differences among different genera (EDX and elemental mapping, AF unpublished data). This result is not surprising because most organic tissues in weathered conditions, not only of brachiopods, but also of other fossil groups are replaced by iron minerals in this type of fossil Lagerstätte, except when organic remnants are preserved. Iron minerals completely replicate the morphology of the soft-parts and are present as single micro-euhedral crystals and framboids. SEM analyses on iron mineral crystals (Fig. $10F_2$) of a *Lingulellotreta* from Xiaolantian with preserved soft-tissue show a difference in crystal size and morphology inside the shell (Fig. $10F_1$, F_3, F_6) and within the pedicle (Fig. $10F_1$, F_4, F_7). The crystals of the visceral area appear to be well developed and bigger than those of the pedicle, where they did not develop completely or have been removed. In the region shown in Fig. $10F_1$: position 4 and enlarged in $10F_5$, the shell appears without any crystals at all, and some pores are visible on the shell surface.

Soft-tissue mineralization in modern linguliform brachiopods.—Multiple analyses have been performed on several Recent linguliform brachiopods to gain information about the composition, structure and position of lophophore, nephridia, pedicles, gut wall, and muscles. Furthermore, this dataset has been compared with data gained from histological sections and computed tomography to address differences in fossilization potential. In *Lingula*, the gut is located in the visceral cavity like the majority of the organs. The gut is U-shaped (Fig. $2B_1$) with the anterior mouth at the centre of the lophophore (Fig. $2B_2$). Its wall comprises 3 layers: the inner epithelium is made of very long single cells, the median layer consists of connective tissue, and the external epithelium is composed of flat cells (Fig. $2A_4$, A_6). The gut wall reveals a mixed mineralogical composition of silicon, calcium and phosphorus, and organic compounds (Fig. 11A). The guts of several individu-

← Fig. 3. Elemental mapping of linguliform brachiopod shells; green for P (A_1–H_1), pink for Ca (A_2–H_2). **A**, **B**. Linguliform brachiopods (AF Shi 4-0818, AF Shi 4-0815b, respectively) from Cambrian Guanshan Fauna, China. **C**, **D**. Linguliform brachiopods (AF Hai 4-083, AF Hai 4-085, respectively) from Cambrian Chengjiang Fauna, China. **E**. Recent *Lingula anatina* Lamark, 1801 (AF JEn.An.Long) from Japan. **F**. Recent *Lingula anatina* Lamark, 1801 (MS-Ch.L.an) from China. **G**. Recent *Lingula adamsi* Dall, 1873 (MS-Ch.L.ad) from China. **H**. Recent *Glottidia albida* (Hinds, 1844) (AF Cal.G.al) from California.

Fig. 4. BSD image of a Recent lingulid brachiopod *Glottidia albida* (Hinds, 1844) (AF Cal.G.al) from California. **A**. Complete specimen. **B**–**E**. Details of the shell layers (frame in A). Elemental mapping: pink for Ca (**B**), green for P (**C**). **E**. Detail of D, visible the reticulate pattern of the organic layer. →

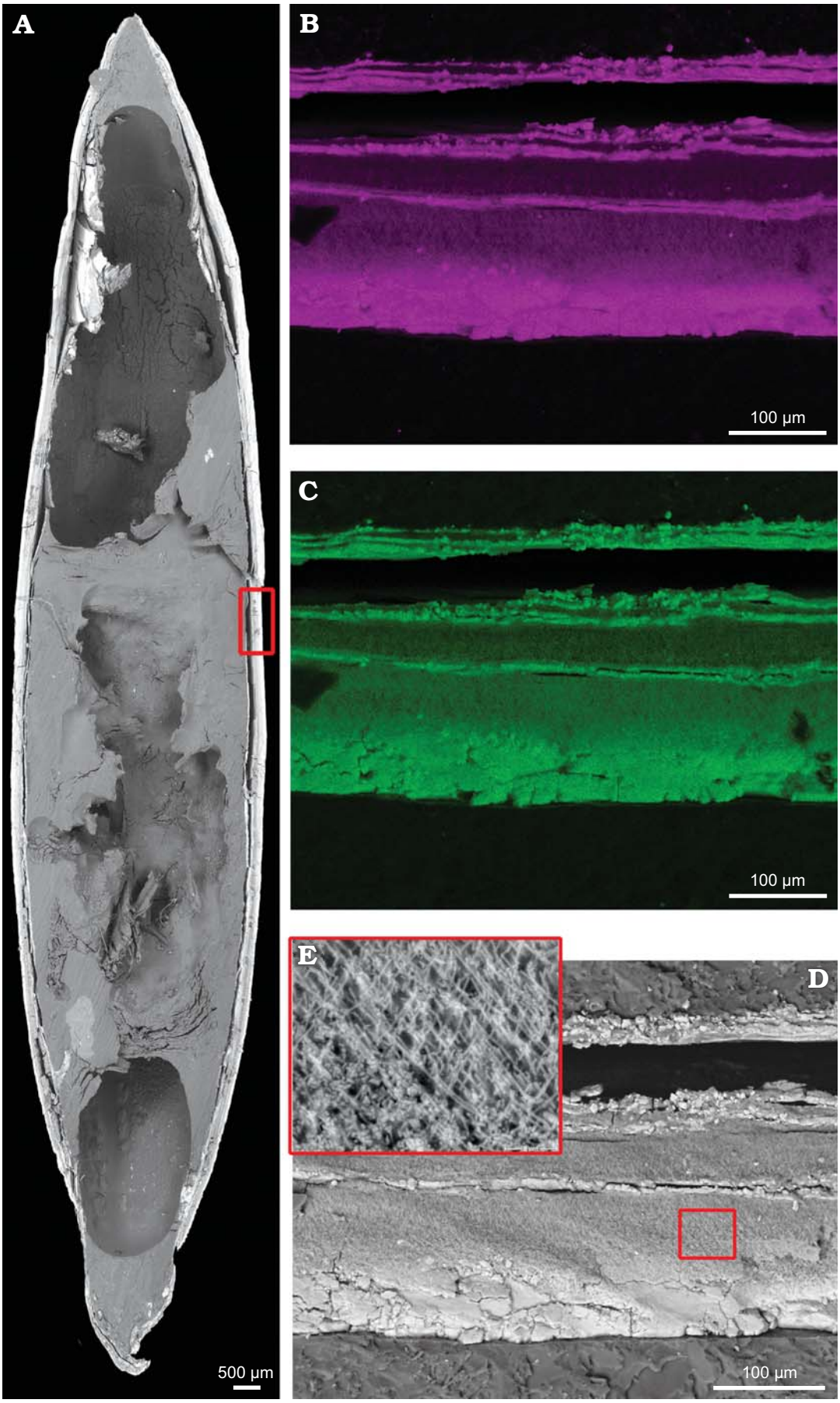

http://dx.doi.org/10.4202/app.2011.0182

als of *Lingula anatina* and *L. adamsi* show the presence of diatoms, which in a single case (a *L. anatina* from Japan) are dissolved and formed a compact layer of Si placed on the inner side of the gut wall (Fig. 11B). The brachiopod lophophore consist of two brachia, connected with each other at the midline (Fig. $2B_2$). They occupy most of the space in the mantle cavity. The volume of the visceral cavity of the linguliform brachiopods seems to have increased from the Lower Palaeozoic to the Recent, whereas the volume occupied by the lophophore has decreased. The lophophoral tentacles bear two types of cilia (Fig. $2A_1$, A_2). Frontal cilia on the inside face of the tentacles extend into the interior of the lophophore, whereas lateral cilia on the sides of the tentacles extend into the gap between adjacent tentacles. Analyses performed on *L. anatina* reveal a silicon impregnation (probably silica as visible from the point analysis) in the lophophore (Fig. 11C). Results of the composition of lophophore analyzed with EDX were compared with those gained from histological sections. The lophophore consists of connective tissue which is covered externally by an epidermis and internally by a coelomic epithelium, both of which are underlain by a basement membrane (James et al. 1992). Histochemical studies (James et al. 1992) suggest a similarity between the globular inclusion bodies in the lophophore of *L. anatina* and those found in the outer mantle epithelium, used as storage tissue. The lacunae of the connective tissue of the lophophore may also be repositories for storage material (James et al. 1992 and references therein). EDX analyses show the diffuse presence of silicon in the whole lophophore, not only located in a specific part, tissue or layer (Fig. 11C).

The pedicle is a long muscular extension of the body used to anchor the animal in its burrow. It consists of a central coelomic canal, a coelomic epithelium, a ring of muscular tissue layer that fills most of the interior of the pedicle, and an external thin layer of connective tissue. The pedicle emerges from between the narrow posterior ends of the valves, but there is no special aperture for it in inarticulate species. In *Glottidia* and *Lingula* the connection between the pedicle coelom and the trunk coelom remains open through life (Fig. $2A_5$). Elemental mapping carried out on the pedicle show the presence of silicon, filling the coelom, and traces of sulphur and potassium (Fig. 12). In extremely rare cases mud infills have been observed in the pedicle coelom of *Lingulella chengjiangensis* from the Chengjiang fossil Lagerstätte. Additional information has been collected for nephridia and periostraca. In the organo-phosphatic inarticulate brachiopods the periostracum is made of protein and chitin (Williams 1968). Analyses of *L. anatina* from Japan (Fig. $2C_2$) and *L. adamsi* from China show their external layer to contain iron enrichments, probably due to iron minerals which often adhere on its external surface, or related to the presence of melanin or some iron storage proteins. A large metanephridium lies on each side of the body cavity with their proximal ends protruding from under the muscles to the trunk coelom. The nephridia are made of three different layers (Fig. $2A_4$, A_6). In *L. anatina* the nephridia also indicate an iron enrichment (Fig. $2C_1$) due to resorption of coelomic fluid which contains coelomcytes with hemerythrine as an oxygene-binding protein.

Geochemistry.—Elemental mapping and EDX analyses of Cambrian linguliform brachiopods reveal distinct differences between unweathered and weathered fossil specimens: elemental mapping of scarcely or not weathered material reveals significantly different amounts of calcium, phosphorus and carbon in the fossils. Weathered fossil material shows iron oxide and hydroxide minerals; however, elemental mapping of those specimens reveals a lack of organic matter and apatite (Fig. 13). Analyses of linguliform brachiopods (*Lingulella* and *Lingulellotreta*) of the Guanshan and Chengjiang Biotas show no evidence of pyrite in the unweathered shell. Sporadically, pyrite crystals were found in the matrix of the Chengjiang material, whereas pyrite minerals were more frequent in the matrix of the Guanshan material. Weathered fossils mostly revealed complete dissolution of original biominerals such as apatite, but often still retained a carbon frame on which iron phases were precipitated. The iron phases occurred as framboids, single octahedral crystals, or spherical aggregates. Occurrence of Fe crystallites and framboids on soft-tissues and within dissolved skeletal parts reveals a later diagenetic origin or even latest replacement during relatively recent weathering. Unweathered samples with contents in TOC of 0.2–0.4 wt% reveal that pyrite is uncommon, mostly dispersed within sediments, and usually not concentrated on soft-tissues or skeletal parts. Redox parameters for least-weathered samples from Yu'anshan Formation do not indicate deposition under anoxic conditions ($U_{authigen}$ # 2.4; V/Cr = 1.9–1.0; Fe_{HR}/Fe_{TOT} = 0.36–0.27). It can be inferred that bottom-water anoxia was not permanently present during deposition of Yu'anshan Formation. Rapid deposition in finest claystone is here considered to be important for the preservation of highly decayable tissues, as already suggested by Conway Morris (1986, 1989) for Burgess Shale, because sediments were oxygenated, presence of bioturbation has been proved (Weber et al. 2012) and also the geochemical proxies do not show persistent anoxic conditions, even though bottom water anoxia and microbial sealing may further increase the probability of soft-tissue preservation via fast and undisturbed embedding in clastic sediments.

Results based on elemental mapping of sponges (Forchielli et al. 2012), brachiopods (this work) bradoriids, arthropods, and worms from the Guanshan Fauna (Forchielli unpublished data) allow us to consider the preservation of the

Fig. 5. BSD images of Recent lingulid brachiopods. **A**. *Lingula adamsi* Dall, 1873 (MS-Ch.L.ad) from China. **B**. *Lingula anatina* Lamark, 1801 (AF JEn.An.Long) from Japan. Complete specimens with soft parts (A_1, B_1). Elemental mapping of the shell fragments (frames in A_1, B_1): Ca (pink) (A_2, B_2), P (green) (A_3, B_3), and Fe (blue) (A_4, B_4). Notice the difference in the number of organo-phosphatic layers between the two species, measured for both below the median adductors. →

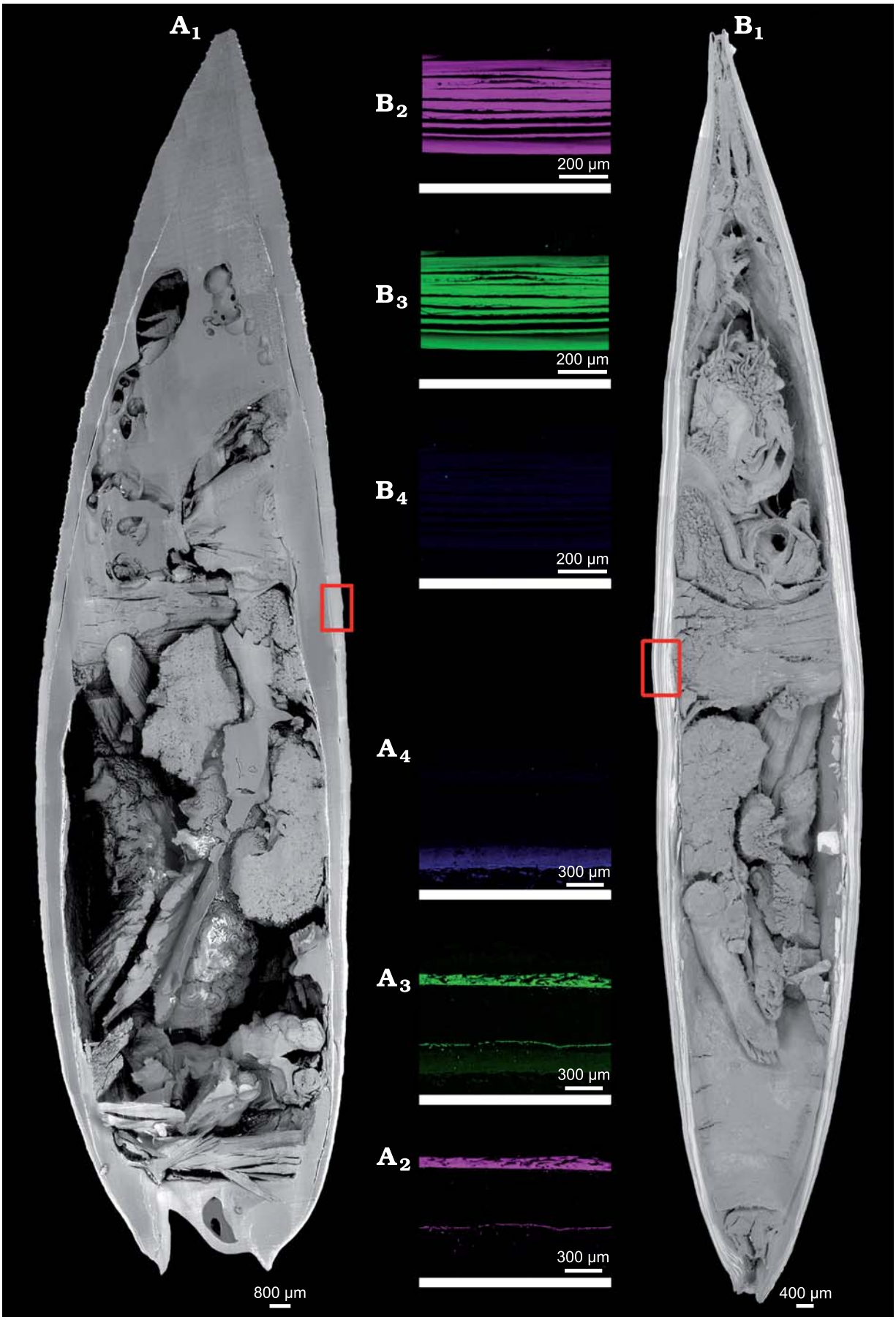

http://dx.doi.org/10.4202/app.2011.0182

Guanshan Fauna to be similar to that of the Chengjiang Fauna. Furthermore, the mechanical behavior of the claystone is similar for both Lagerstätten; unweathered material, as well as wet weathered material, does not easily split along bedding planes, making it difficult to find fossils.

Discussion

Analyses of the structure and composition of the primary shell layer show different results than Emig (1990) and focus on the problematic issue of integration of palaeontological and biological datasets necessary to interpret the linguliform brachiopod shell. Furthermore, our analyses clearly document the difference between the various species of the genus *Lingula* in the amount of apatite present in the shell. The shell of *Lingula adamsi* also shows platy siliceous structures and ferromanganese precipitate that are absent in *L. anatina*. The Si-rich structures may be related to similar silicon tablets reported by Williams et al. (1998, 2001) for *Discinisca*. The presence of ferromanganese precipitate with minor content of apatite is reported to have a bacterial origin in the shells of several freshwater and marine molluscs (e.g., Swinehart and Smith 1979 and references therein). The presence of Mn precipitate in the shell of the living *L. adamsi* might also have a bacterial origin, also related to the partial transition between oxic and dysoxic environments in the burrows of these linguliform brachiopods. Significant differences in the organic constituents of the respective species have already been stated by Jope (1977) and Iijima and Moriwaki (1990); our study on apatite content and the cited previous studies pointed out the existence of differences between *L. anatina* and *L. adamsi* therefore, the genus should not be analysed at generic level (*Lingula*) but at the specific level in future studies of brachiopod shells. Iijima and Moriwaki (1990) argued that *Lingula* shells contain a large amount of alanine (glicine/alanine = 0.42–1.48). According to Iijima and Moriwaki (1990), such a difference suggests a correlation between components of structural protein and apatite. The genus *Glottidia* shows almost uniform values of apatite along the longitudinal shell section, whereas the two species of *Lingula* exhibit a decrease in the apatite amount in the anterior end where the setae are located, and a maximum in the region of the median adductors, relating the thickest part of the shell to the location of the main muscle. Initial analyses of a pelagic juvenile of *L. anatina* with 9 pairs of tentacles show that, at this ontogenetic stage, the shell appears to consist entirely of organic material and lacks apatite or other mineral enrichments. This observation requires further confirmation from more and unfixed stages of lingulid larvae. However, the first formation of apatite layers in the shell seems to occur when the larva settles and begins an infaunal life style.

Elemental mapping and BSD and EDX analyses of unweathered shells of linguliform brachiopods from the Chengjiang and the Guanshan fossil Lagerstätten reveal a primary multilayered organ-phosphatic composition with tubules penetrating the biomineralized layers. A similar structure was also observed for linguliform brachiopods of the Siberian Sinsk Biota. Here the high individual abundance (169 specimens or 47.9% of individuals) reveals brachiopods as the dominant metazoan group in this biota (Ivantsov et al. 2005), and all our specimens showed a pristine layered structure. This finding indicates that earliest crown-group brachiopods developed organo-phosphatic skeletons, comparable to modern linguliform brachiopods (Fig. 3), by Cambrian Stage 3. This characteristic is observable only in optimally preserved material (i.e., minimally affected by weathering or diagenetic alteration) because in the weathered material the original shell is replaced by iron minerals and diagenetic alteration resulted in complete apatite replacement. The principal preservation in the two Yunnan Lagerstätten shows that the skeletal and soft-tissues of brachiopods in (mostly weathered) fine mudstone are replaced by iron oxides and hydroxides. In contrast to the distal marine depositional environment of the Chengjiang deposit, deposition in the Wulongqing Fm. (Guanshan Biota) occurred in shallower water settings with the presence of storm deposits (Luo et al. 2008). It is remarkable to note that soft-tissue remains also occur in bioturbated beds: bioturbation is everywhere in all levels of the Wulongqing Formation (Weber et al. 2012). Weathered fossils mostly revealed complete dissolution of original biominerals, such as apatite, but often still retained carbonaceous remains upon which iron phases were precipitated. The iron phases occurred as framboids, single octahedral crystals, or spherical aggregates. The occurrence of Fe crystallites and framboids on soft-tissues and within dissolved skeletal parts reveals a later diagenetic origin or even latest replacement during relatively recent weathering. Iron incorporation in organic tissues of modern *Lingula* is more pervasive than previously reported. It is observable in different tissues such as in the periostracum and nephridia. There are several hypotheses for its presence in living linguliform brachiopods. Ferritin is a protein that stores iron and is produced by almost all living organisms. A ferritin subunit (soma ferritin) is associated with shell formation in the pearl oyster (Zhang 2003). A similar process in the *Lingula* periostracum, composed entirely of protein and chitin, may explain the iron presence. Another protein often described in the context with the oxidation and ligation states of the iron centre is hemerythrin, a nonheme iron containing the equiva-

Fig. 6. Mineralization in the external layer of lingulid brachiopod Recent *Lingula adamsi* Dall, 1873 (MS-Ch.L.ad) from China. **A**. BSD image of one of the "pockets" of the external layer. The red arrow points to the ferromanganese precipitate enlarged in G; the red dot indicates the siliceous platy structure analyzed in B. **B**. Point analysis of the platy structure of the pocket. **C**–F. Elemental mapping of the area shown in A: Si (yellow) (**C**), Al (red) (**D**), Mn (turquoise) (**E**), Fe (blue) (**F**). **G**. A close up of a ferromanganese precipitate, the concentric structure is visible. **H**–**J**. The point analyses carried out on different layers of the nodule. →

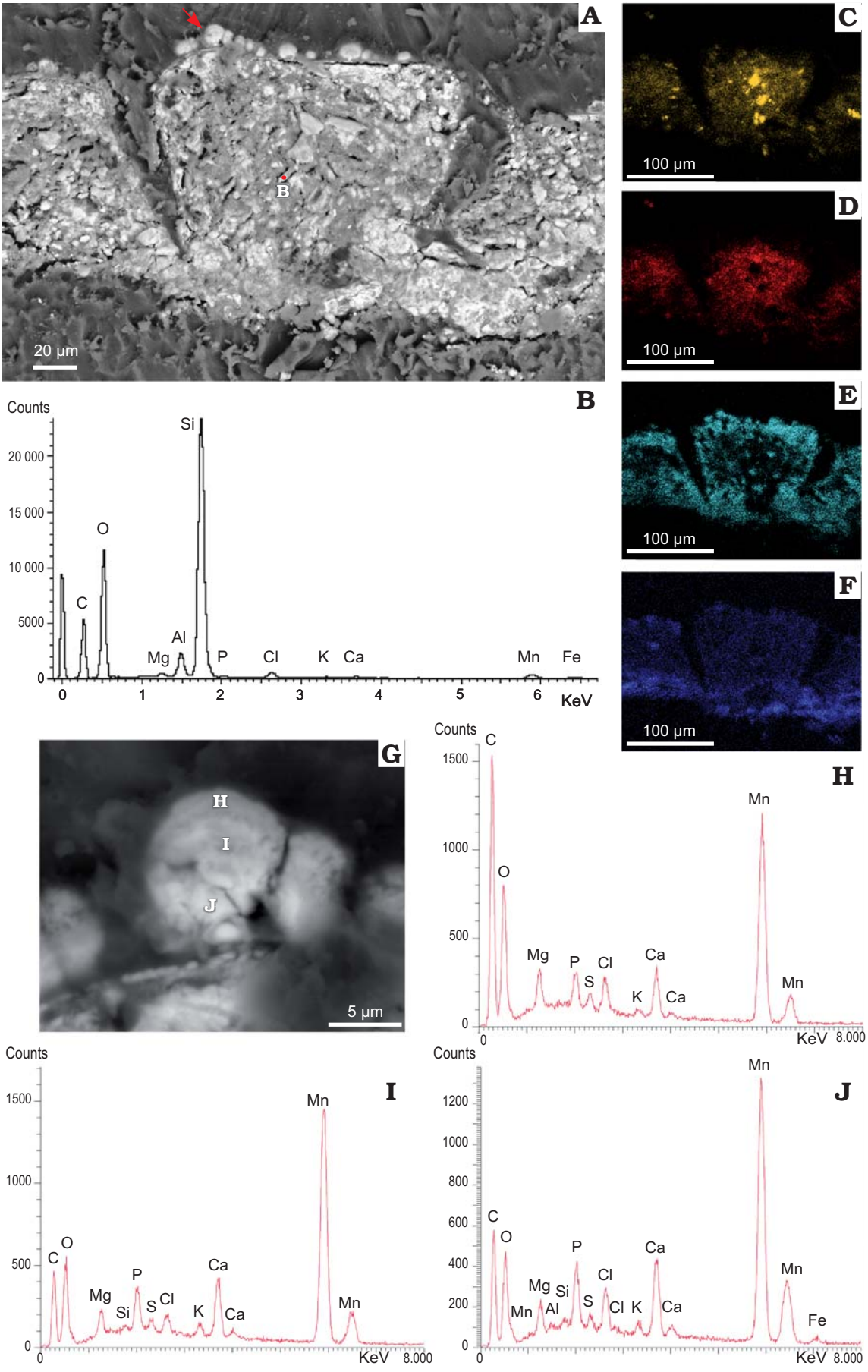

http://dx.doi.org/10.4202/app.2011.0182

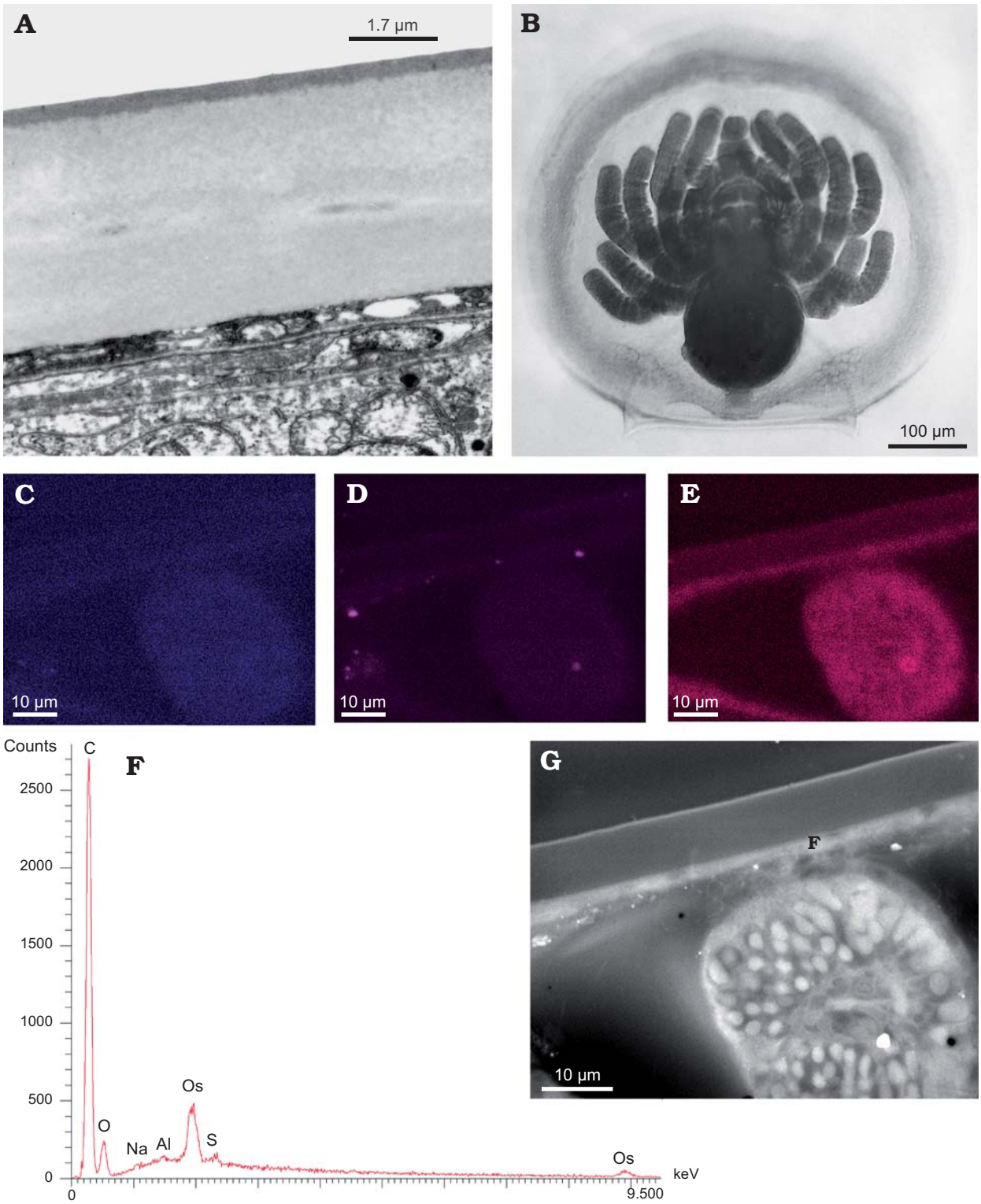

Fig. 7. Analyses of a juvenile specimens of Recent lingulid brachiopod *Lingula anatina* Lamark, 1801 from Australia. **A**. TEM image of juvenile specimen. Longitudinal section through the mid juvenile shell and underlying mantle tissue. The shell material is unstructured apart from a more electron dense outer layer. **B**. Light microscope image of a ventral view of a pelagic juvenile specimen with 7 pairs of tentacles. Specimen in liquid embedding resin after glutardialdehyde and OsO_4 fixation. **C**–E. Elemental mapping of area shown in G: Fe (**C**), Ca (visible Ca granules) (**D**), Os (**E**). **F**. Point analysis of the whitish electron-denser layer (area shown in G), 1.8 µm thick of the shell of G. **G**. BSD image of a longitudinal section.

lent of haemoglobin (Manwell 1960). It is a protein responsible for oxygen transport in sipunculids, priapulids, brachiopods, and annelid worms. It can be used as an oxygen carrier protein in brachiopods also. Another hypothesis for the presence of iron in the periostracum is the colour pattern on the shells. This results from different types of pigment deposited

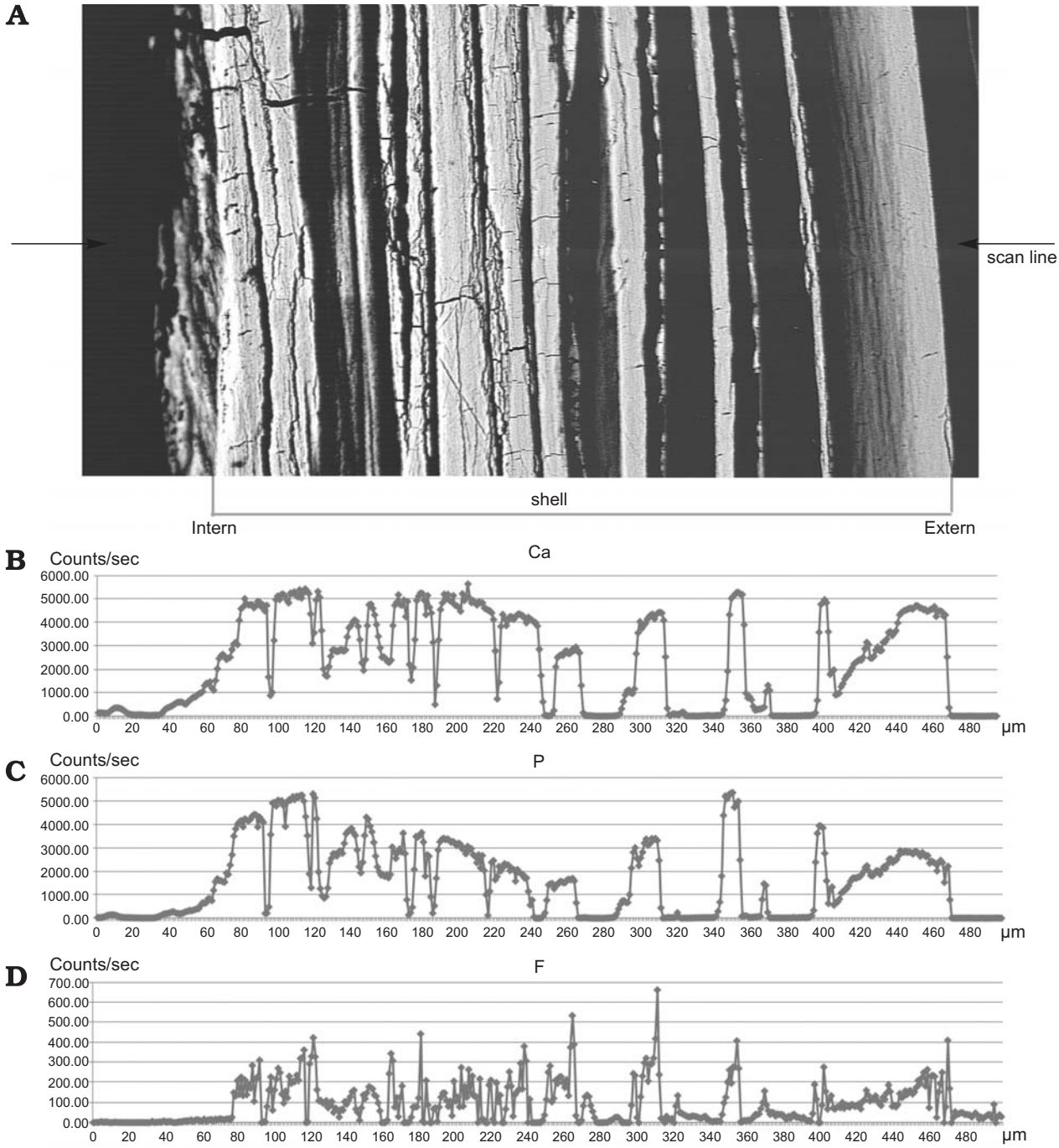

Fig. 8. Microprobe WDS scan line of Recent lingulid brachiopod *Lingula anatina* Lamark, 1801 (AF JL.An.Tra) from Japan. **A**. Shell section, the length of the portion measured is about 500 µm, and has been taken below the median adductor muscle. Ca (**B**), P (**C**), and F (**D**) are plotted according to the procedure described in the material and methods section and are concordant with fluorapatite mineral.

within the shell layers, principally the periostracum (Kriz and Lukes 1974). Melanin is one of the most common pigments in shells (Comfort 1951) and is reported also in fossil brachiopods (Kriz and Lukes 1974). In animals, melanin pigments are derivatives of the amino acid tyrosine. Modern inarticulate brachiopods generally display dark colours such as brown (Kobluk and Mapes 1989), even if most of our *L. anatina* specimens show a brilliant light green colour. In the Brachiopoda, it is supposed that shell pigments are secreted by epithelial cells of the mantle as waste of the completed metabolic functions or as a product of cell metabolism (Kriz and Lukes 1974). Some brachiopods show colour patterns that may not be due to pigmentation, but rather to the structure of the shell itself (Kobluk and Mapes 1989). It seems likely that the presence of iron in living linguliform brachiopods is linked to some protein of the brachiopods themselves or to some external influences; the iron revealed by EDX analyses in the nephridia is related to the absorption of sub-

http://dx.doi.org/10.4202/app.2011.0182

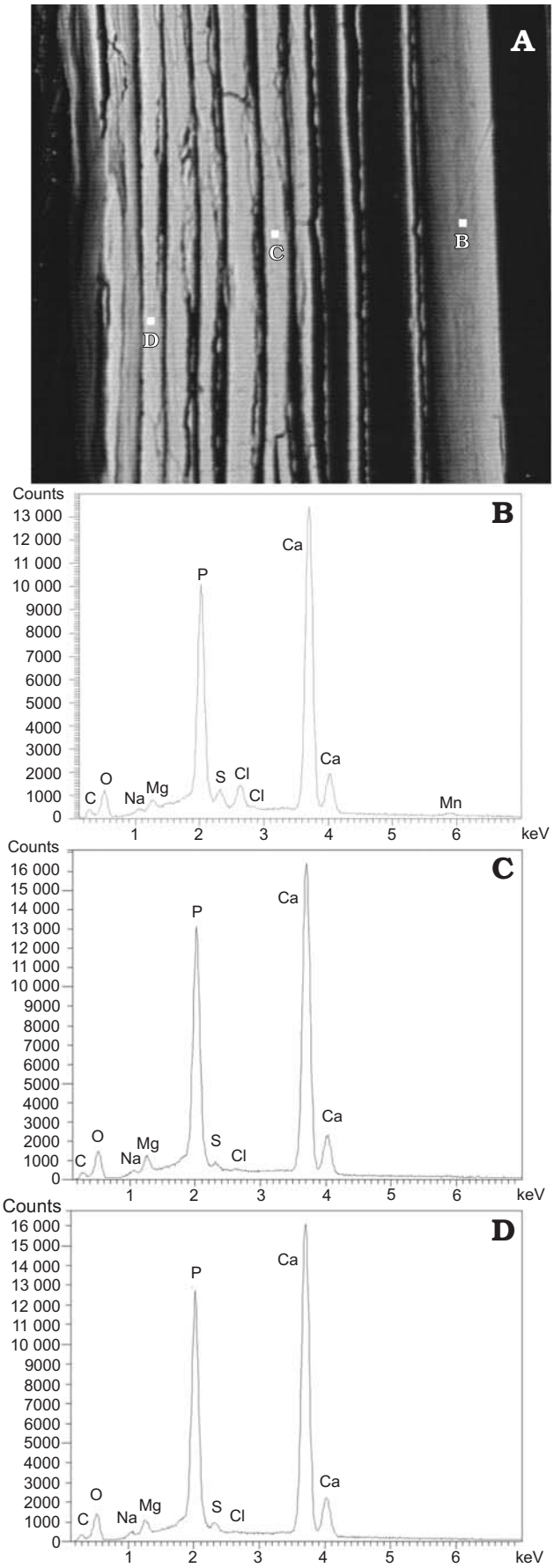

stances from the coelomic fluid, containing hemerythrin, whereas the iron analyzed in the periostracum which is composed in *Lingula* of protein with an elevated pyrrolidine-amino acid content (Jope 1969) and chitin (Williams 1968) is probably related to some proteins too, but the influence of the seawater or embedding sediment iron content on the external layer cannot be ruled out. Swinehart and Smith (1979) report iron and manganese in the periostraca of several bivalve mollusks. In their samples, the metals are located towards the outer surface of the periostracum. They argue for a possible bacterial origin of this metal enrichment: the presence of manganese (exchanged with Ca^{2+}) and iron associated with phosphate and protein produces a condition which can maximize their nutritive availability to microorganisms. In our sample there is iron not only inside the Mn precipitate (Fig. 6A), but also on the external surface of the periostracum, a bacterial origin of the ferromanganese precipitate, indeed, may be possible, however, as in seafloor ferromanganese nodules and crusts there also appears the possibility that Fe and Mn are precipitated onto an organic matrix and grow autocatalytically at an interface between oxygenated and oxygen depleted waters. Remarkable also is the presence of apatite in the ferromanganese precipitate in the outer shell of *L. adamsi*, since here a different mechanism to precipitate apatite in the lingulid shells appears to act. The precipitation of ferromanganese precipitate associated with apatite is not an active, genetically triggered biomineralization. Active FeMn biomineralization is very rare in invertebrates and often it is associated to bacterial activity (e.g., Tazaki 2000). The specific location of Fe and Mn only in the part of the shell which is exposed to sea water may suggest influences by the chemocline or bacterial activity, but the localization does not suggest active biomineralization. In contrast to this it appears most likely that the ordinary lamellar apatite formation within the shell of *Lingula* is directly controlled by biochemical processes of the organisms, because the number and thicknesses of apatitic layers vary due to functional differences in the shell regions and organ arrangement.

← Fig. 9. Microprobe EDS analyses of Recent lingulid brachiopod *Lingula anatina* Lamark, 1801 (AF JL.An.Tra) from Japan. **A**. Shell section. The external (**B**), median (**C**), and internal (**D**) portions of a valve of the shell. Measurements were made below the median adductor muscle.

Fig. 10. Soft tissue preservation in Cambrian linguliform brachiopods. → **A**. *Lingulella chengjiangensis* Jin, Hou, and Wang, 1993 (Maf-b-50b) from the Chengjiang Biota; fossil pedicle preserved; the central coelom is visible as a dark line in the middle part of the pedicle. **B**, **C**. Lophophora and visceral area in two different specimens: *Acanthotretella decaius* Hu, Zhang, Holmer, and Skovsted, 2010 (GKG-008b) from the Guanshan Biota (**B**) and *Lingulellotreta malongensis* Rong, 1974 (Maf-b-245) from the Chengjiang Biota (**C**). **D**. *Lingulella chengjiangensis* Jin, Hou, and Wang, 1993 (Maf-b-50a) from the Chengjiang Biota with soft tissue preserved; the coelom is visible in the median part of the pedicle. **E**. *Acanthotretella decaius* Hu, Zhang, Holmer, and Skovsted, 2010 (GKG-008a) from the Guanshan Biota with soft tissue preservation. **F**. *Lingulellotreta malongensis* Rong, 1974 (MS-XLTped) from Xiaolantian, Cambrian (F_1); elemental mapping of Fe (F_2); details of areas shown in F_1 (F_3–F_7).

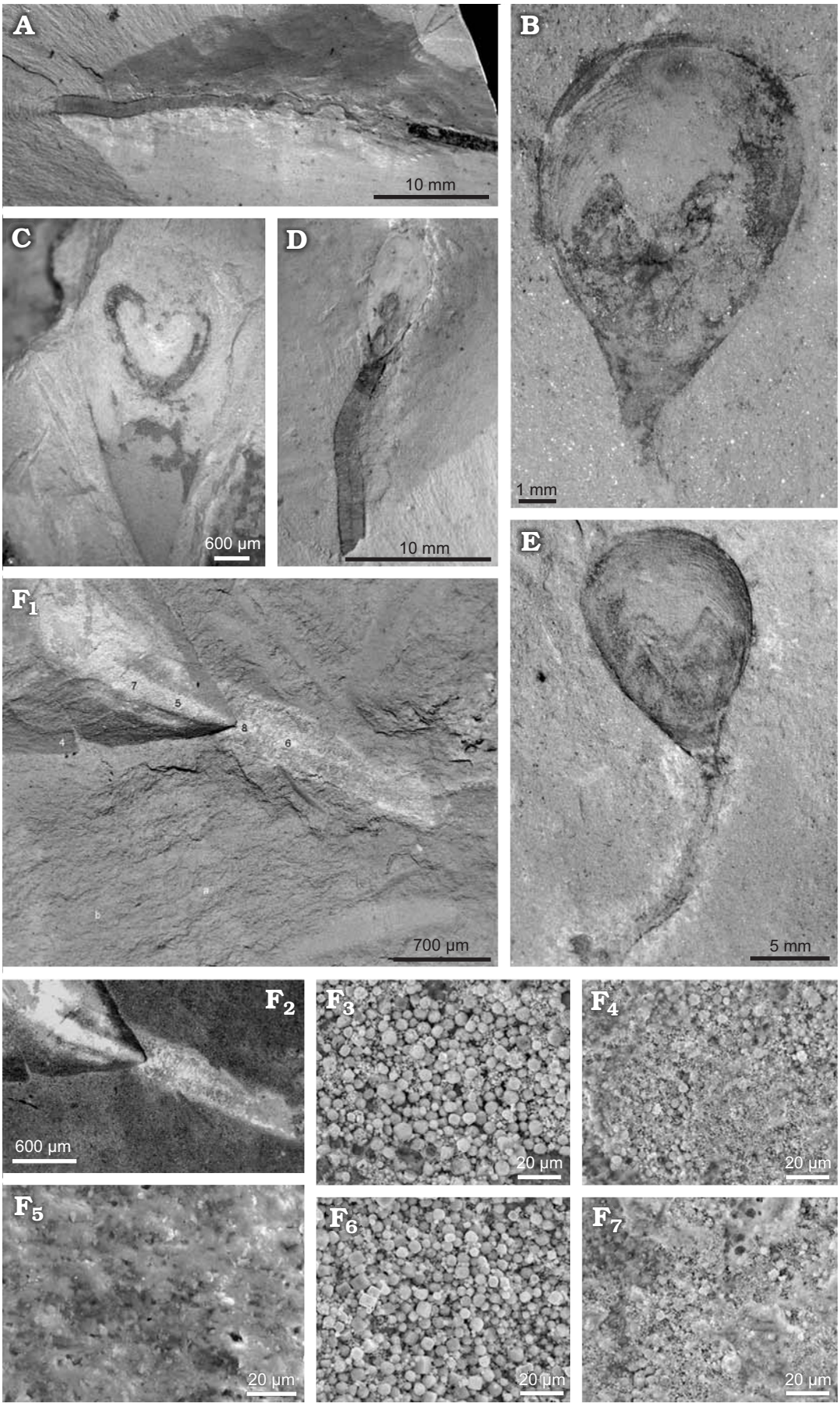

http://dx.doi.org/10.4202/app.2011.0182

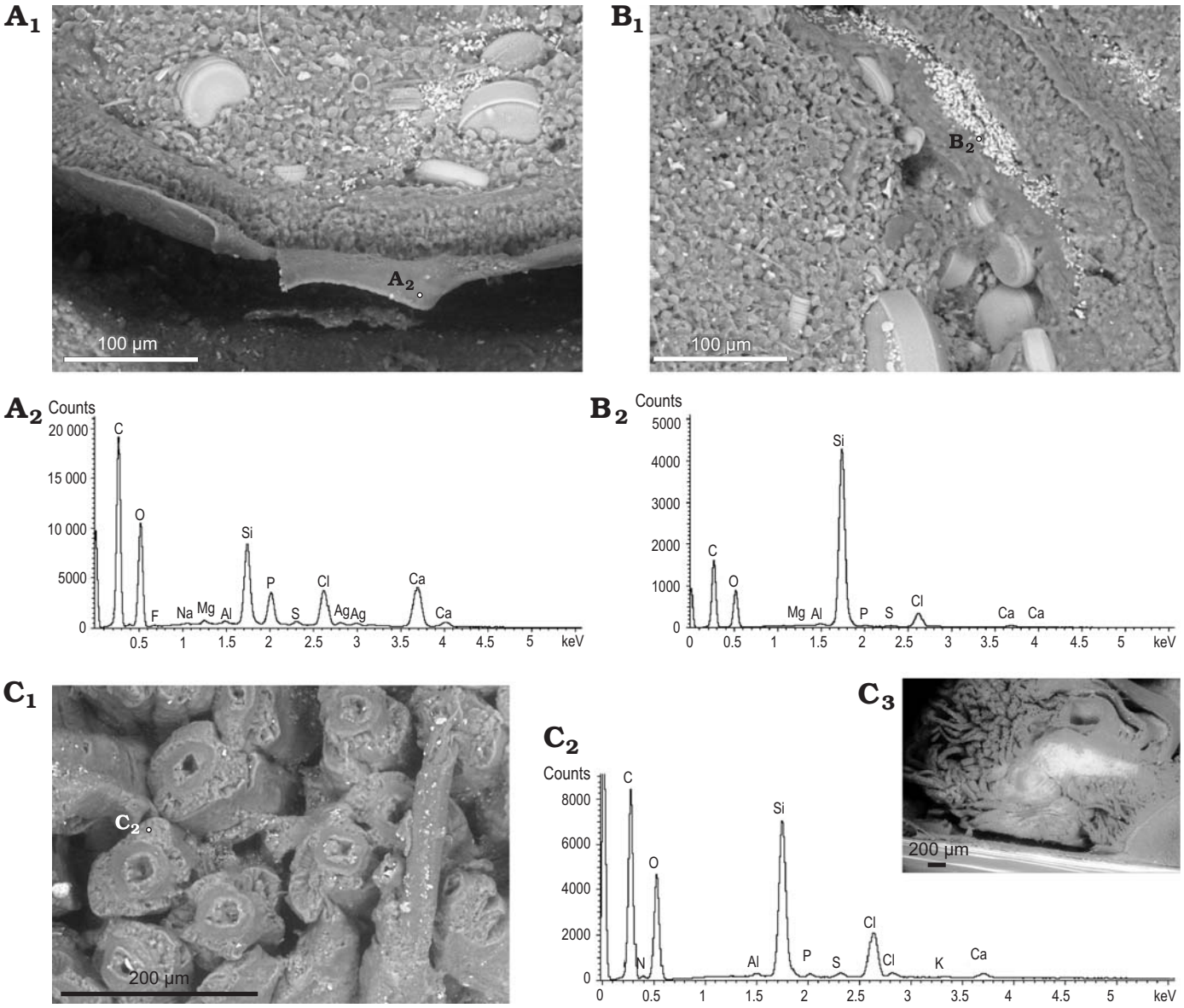

Fig. 11. EDX analyses of Recent lingulid brachiopod *Lingula anatina* Lamark, 1801 (AF JEn.An.Long) from Japan. **A**. The gut wall. **B**. The gut content with the siliceous layer due to the diatoms. **C**. The lophophore (C_3), close up of the lophophoral tentacles (C_1). The white mineral visible in C_1 and C_3 is Si (distributed in the whole lophophore). SEM photographs (A_1–C_1, C_3), EDX point analyses (A_2–C_2).

Preferential preservation of some brachiopod soft-parts also occurs in the Chengjiang Lagerstätte of Yunnan. Lophophores, guts, and pedicles are often preserved as iron oxides or are preserved in 3D by clay. Data reported in Zhang et al. (2003a, 2004a, b, 2005, 2007, 2008b), mostly concerning *Lingulellotreta malongensis* and *Lingulella chengjianensis*, show preferential preservation of lophophores (no data are available about pedicle preservation). The volume of the visceral cavity of the Chengjiang linguliform brachiopods is relatively small, compared to those of their extant representatives. Lophophores show an elevated content of silicon in living specimens of *Lingula* and an iron mineral replacement in fossil linguliform brachiopods. James et al. (1992) suggested that some tissue in the lophophore might act as storage tissue if the storage was intended for organic compounds that store iron; with decomposition it might be released, forming diagenetic minerals. The silicon in living *Lingula* comes from the surrounding environment; the mucus present in the lophophore can drive silicon from the outside into the organ. Silicon is an inert element; it is not related to any organic compound. An external origin for the silicon in these organs is therefore extremely probable in both living *Lingula* and in Cambrian linguliform brachiopods. A study of fossil linguliform brachiopods from Chengjiang County by Jin et al. (1993) suggests a lack of significant changes in the structure and function of the pedicle through time. They argued that the comparison of specimens collected from different geographical areas through Palaeozoic outcrops shows that the delthyrial area to which the

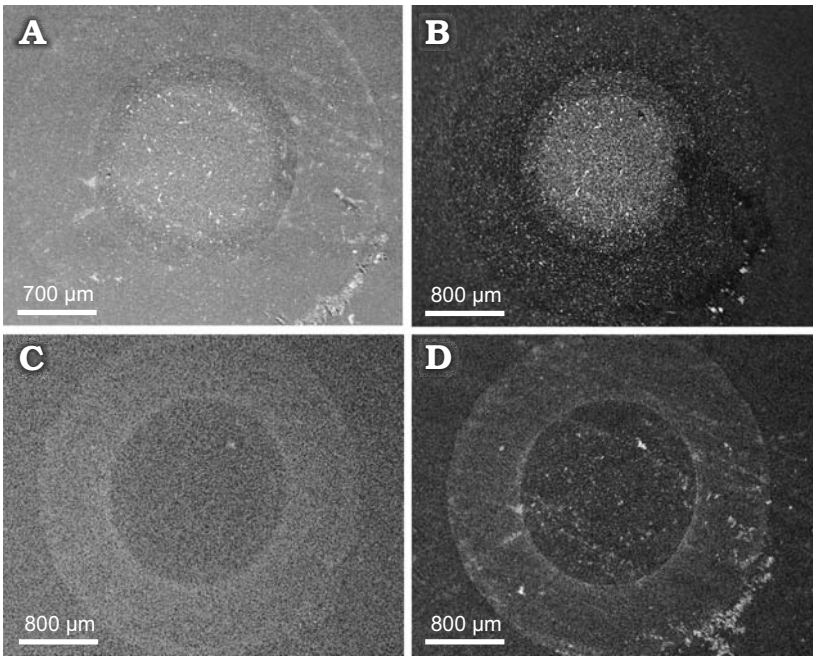

Fig. 12. BSD and elemental mapping of the pedicle of Recent lingulid brachiopod *Lingula anatina* Lamark, 1801 (AF JL.An.Tra) from Japan. **A**. BSD image. **B**. Elemental mapping of Si (K alpha), indicate enrichment in the coelom. **C**. Elemental mapping of S, from the position it is related to muscle masses. **D**. Elemental mapping of K, showing traces in the connective tissue layers.

pedicle muscles are attached was reduced since the Cambrian until these muscles were completely embraced by the two valves, and that in some specimens the end part of the pedicle showed a reduction of the muscle thickness that could be related to the similar characteristic present in the Recent *Glottidia*, where the reduction of the chitinous part permits the collection of sand grains or mud (Mackay and Hewitt 1978). The silicon and the sulphur present in the pedicle could be due to external influences of the living environment. The sulphur may have two origins: it could be related to iron sulphides connected with the partial transition between oxic and dysoxic environments of the burrows in which this invertebrate lives, or more likely to the aminoacids of the pedicle itself. The study by Williams and Cusack (1997) on Carboniferous lingulids from Scotland provides evidence of the differential mediation of various organic constituents in clay formation. They argued that GAGs degraded during fossilization (facilitating the diffusion of pore fluid solutes such as silica and alumina throughout the shell) without disturbing apatitic ultrastructures, and the space so created became filled with sheets of recrystallized apatite with kaolinite. The kaolinite in the shell contrasts with the illite of the entombing sediment and suggests that degrading acidic GAGs mediated in clay formation in situ (Williams and Cusack 1997). Furthermore, it was stated that Lower Carboniferous strata of Scotland also contain framboidal pyrite, which is absent from the shells themselves. This imbalance supports mediation by another gel, the glycocalyx, secreted by the inner epithelium of the brachiopod mantle. The glycocalyx would have lined the shell interior and could have served as sorption film for dissolved metals precipitated as compounds on decomposition of body tissue (Williams and Cusack 1997). A similar scenario might be possible for the Cambrian Lagerstätten of Yunnan too; here the embedding sediment is rich in illite (Gabbott et al. 2004; Forchielli et al. 2013), and pyrite is also present in sediment but absent from unweathered fossil shells.

Our preservational hypothesis for soft-tissued lingulid fossils is strongly related to clay minerals: we consider a rapid deposition of finest claystone to be a crucial factor for soft-tissue preservation. Furthermore, the presence of silicon in some organs and shell layers of modern linguliform brachiopods can be related to their preferential preservation in the fossil material. A comparison made using different techniques (EDX analyses, microprobe analyses and histological sections) shows that there are no strong differences in the composition between the internal organs of living linguliform brachiopods apart from the position of the lophophore and the pedicle outside the visceral cavity and the related presence of silicon in these two organs, coming from the external environment. Organically bound iron and in-vivo ferromanganese precipitates in some lingulid shells may also enhance the preservational potential for early diagenetic mineral replacements of shells and tissues during fossilisation processes.

Recent specimens of *Lingula* are restricted to littoral and sub-littoral environments. Holocene linguliform brachiopods occur prevalently in nearshore environments, but they are not confined to them; it seems that Palaeozoic linguliform brachiopods did occur in similar environments (Kowalewski and Flessa 1996 and references therein). The geographical distribution of modern *Lingula* is shallow water in Australasia, Africa, Indian Ocean, Japan, China, and Hawaii, while modern specimens of *Glottidia* are relatively common in shallow water along the east and west coasts of North and Central America. Elemental mapping and EDX analyses of several specimens of modern linguliform brachiopods ranging from sub-adult to adult stages from different geographical areas do not show any substantial, geographically based differences in shell composition or, at a species-specific level, in the number of apatite layers.

http://dx.doi.org/10.4202/app.2011.0182

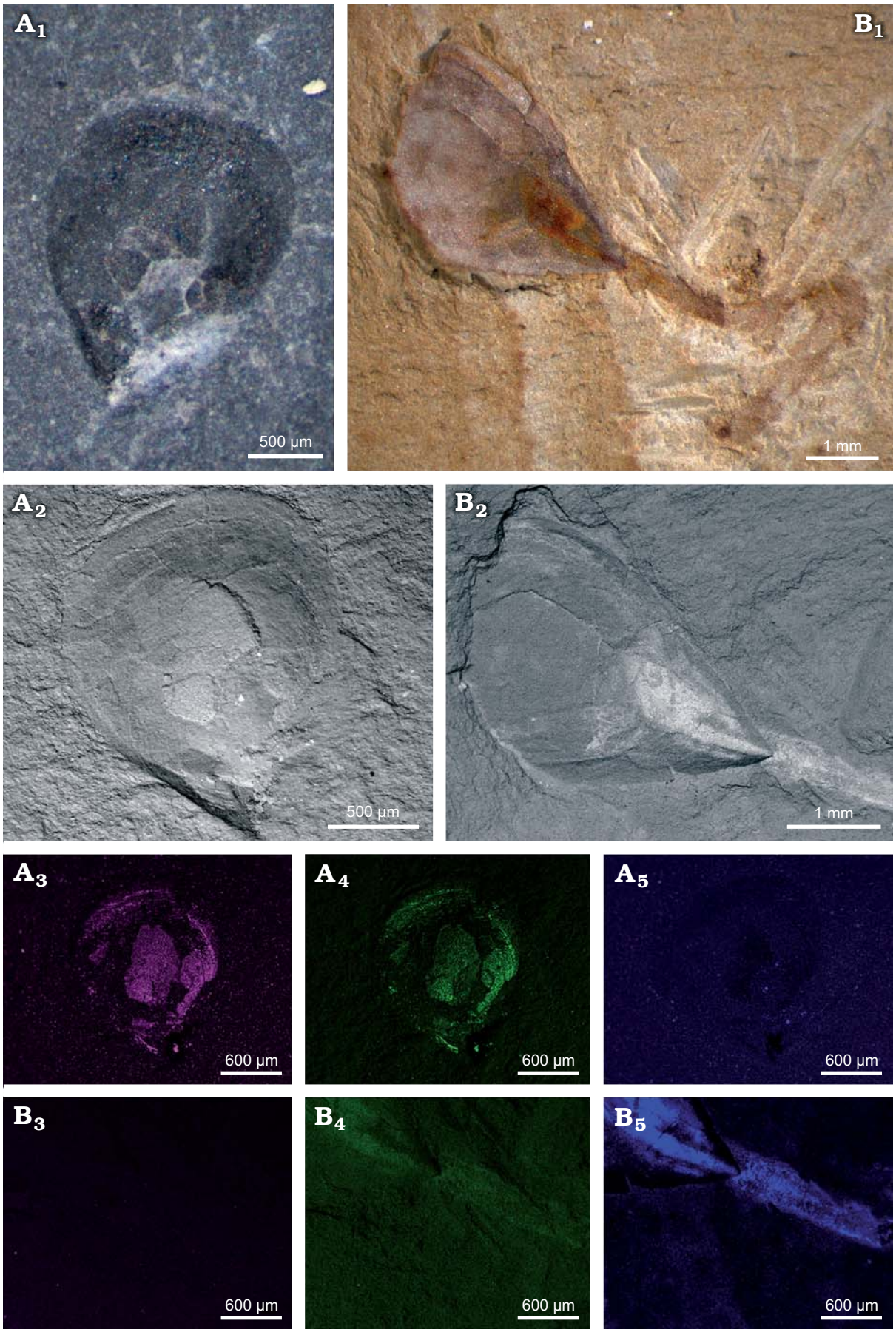

Conclusions

The Chengjiang and Guanshan fossil Lagerstätten are crucial Burgess Shale-type fossil Lagerstätten to understanding the Cambrian bioradiation and widespread exceptional preservation in the Cambrian. It has been supposed that the earliest linguliform brachiopods had organo-phosphatic shells. Our taphonomic analyses of unweathered material confirmed that organo-phosphatic shells were developed at least with earliest crown-group lingulids since Stage 3 of the Cambrian. Multilayered shells, documented in linguliform brachiopods of the Guanshan Biota, of the Chengjiang Biota, and the Sinsk Biota, together with the presence of organic carbon between the phosphatic layers, demonstrate that this material represents an original biological component, and the earliest shell architecture is in principle comparable with those of extant representatives of linguliform brachiopods. Analyses of larval material of modern *Lingula* hint toward a compact and exclusively organic shell during the planktonic stages of larval development. Differences in shell thickness, mineralization grade and apatite content confirmed that the differences between the genus *Glottidia* and the genus *Lingula*, also shown by previous studies on proteins and organic compounds of the shell. Our analyses show a difference at species level in the genus *Lingula* concerning the number of the apatitic layers in the shell, besides the total apatite content, thickness and mineralization grade between the species *Lingula anatina* and *Lingula adamsi*. Furthermore, geographical and environmental influences do not significantly affect the structure and composition of Recent linguliform brachiopod shells. We assume that the same was true for the earliest Cambrian linguliform brachiopods.

The enrichment of some elements such as iron, phosphorus, silicon, and calcium in some organs of living linguliform brachiopods may also account for a differential preservational potential of these organs. Phosphorus uptake and deposition in linguliform brachiopods is still not completely understood. The new recognized pattern of P precipitation in linguliform brachiopods shells (within the ferromanganese precipitate) that may be more influenced by the environment and possibly by bacterial involvement appears in this optic of relevant importance. Silicon was found not only in the lophophore (Fig. 11C), gut (Fig. 11B), and pedicle (Fig. 12B), but also, for the first time, as platy structures in the outer shell of an adult specimen of *L. adamsi*. Analyses of the gut of *L. anatina* and *L. adamsi* show that Si can be dissolved by digestive processes, but if life processes are stopped, it seems to be possible to quickly be deposited (Fig. 11B), Si may then be available for formation of aluminosilicates in geological processes. Aluminosilicates seem to be formed also in the outer shell of modern linguliform brachiopods (e.g., *L. adamsi* in Fig. 6C, D). Si can be excreted in some linguliform brachiopods (larval stage) as Si tablets (Williams et al. 2001) or in similar platy Si structures (our new finding in adult *L. adamsi*). Specific processes that may determine Si dissolution, its transfer into specific tissues and trigger its deposition in the shell may occur in linguliform brachiopods. This may have a considerable influence on the fossilization potential and needs to be further investigated in future. Si precipitation may be a more common phenomenon in linguliform brachiopods than previously recognized. The disposition of the internal organs inside the visceral cavity or outside, in the mantle cavity (e.g., the lophophore), may also be related to the differential preservation of the various organs. Burgess Shale-type preservation does not depend on early iron adsorption. Our new data on modern shell and tissue composition are therefore important for the understanding of preservation in fossil Lagerstätten. It may not only be due to different resistances of organic biomolecules, but also to in vivo binding of specific elements to tissues and parts of the shell as well as post-mortem processes.

← Fig. 13. Elemental mapping differences between weathered and unweathered material. **A**. Unweathered material, linguliform brachiopod (AF Hai 4-083) from Cambrian Chengjiang Fauna, China. **B**. Weathered material, *Lingulellotreta malongensis* Rong, 1974 (MS-XLTped) from Xiaolantian, Cambrian. Light microscope photos (A_1, B_1) and BSD images (A_2, B_2). Elemental mapping of Ca (pink) (A_3, B_3), P (green) (A_4, B_4), Fe (blue-violet) (A_5, B_5).

Acknowledgements

We thank Jörg Nissen for technical assistance with EDX analyses (ZELMI), Jan O. Evers (FU) is also kindly acknowledged for his assistance during photo and graphic work, and David Schmälzle (FU) for sample preparation. We thank Li Guoxiang (Nanjing Institute of Geology and Palaeontology, Chinese Academy of Sciences, Nanjing, China) for joint field work. Recent specimens of *Lingula anatina* from Japan were kindly provided by Kazuyoshi Endo (The University of Tokyo, Japan) and Michitaka Shimomura (Kitakyushu Museum of Natural History & Human History, Kitakyushu, Japan), specimens *L. anatina* from Australia were kindly provided by Mike Reich (University of Göttingen, Göttingen, Germany), and we are thankful to Michal Kowalewski (Virginia Polytechnic Institute and State University, Blacksburg, USA) for *Glottidia palmeri* specimens. We acknowledge Lawrence Och and Graham A. Shields (University College London, UK) for iron speciation analyses. We thank Kazuyoshi Endo and Robert R. Gaines (Pomona College, Claremont, USA) for helpful comments that improved the quality of this manuscript. This study was supported by DFG (Grant No Ke 322/34-1 to AF, MS, HK) National Natural Science Foundation of China (Grant No. 40772020 to SH), and the National Basic Research Program of China (2006CB806401 to SH). Financial support to collect *L. anatina* at Magnetic Island, Australia in 1995 was provided by a DAAD fellowship and DFG grant (Ba1520/1) to CL. This is a contribution to the Sino-German Forschergruppe 736 project "The Precambrian–Cambrian Ecosphere (R)evolution: Insights from Chinese microcontinents".

References

Bengston, S. 2005. Mineralized skeletons and early animal evolution. *In*: D.E.G. Briggs (ed.), *Evolving Form and Function: Fossils and Development*, 101–124. Yale Peabody Museum, New Haven.

http://dx.doi.org/10.4202/app.2011.0182

Blochmann, F. 1900 *Untersuchungen iiber den Bau der Brachiopoden Pt. 2 Die Anatomie von Discinisca und Lingula*. 124 pp. Gustav Verlag, Jena.

Bruguière, J.G. 1797. *Tableau Encyclopédique et Méthodique des trois Règnes de la Nature, Vol.2 : vers, coquilles, mollusques et polypes divers*, 96–314. Agasse, Paris.

Butterfield, N.J. 1995. Secular distribution of Burgess Shale-type preservation. *Lethaia* 28: 1–13.

Butterfield, N.J. 2002. *Leanchoilia* guts and the interpretation of three dimensional structures in Burgess Shale-type fossils. *Paleobiology* 28: 155–171.

Butterfield, N.J. 2003. Exceptional fossil preservation and the Cambrian explosion. *Integrative and Comparative Biology* 43: 166–177.

Chen, J.Y. 2004. *The Dawn of the Animal World*. 366 pp. Jiangsu Science and Technology Press, Nanjing.

Conway Morris, S. 1986. The community structure of the Middle Cambrian phyllopod bed (Burgess Shale). *Palaeontology* 29: 423–467.

Conway Morris, S. 1989. Burgess Shale fauna and the Cambrian explosion. *Science* 246: 339–346.

Comfort, A. 1951. Observation on the shell pigments of land pulmonates. *Malacological Society London, Proceedings* 29: 35–43.

Cusack, M., Williams, A., and Buckman, J.O. 1999. Chemicostructural evolution of Linguloid brachiopod shells. *Palaeontology* 42: 799–840.

Dall, W.H. 1870. A revision of the Terebratulidae and Lingulidae. *American Journal of Conchology* 6: 88–168.

Emig, C.C. 1990. Examples of post-mortality alteration in Recent brachiopod shells and (paleo) ecological consequences. *Marine Biology* 104: 233–238.

Forchielli, A., Steiner, M., Keupp, H., Hu, S., and Li, G. 2009. Taphonomy of Early Cambrian Chengjiang fossils and phosphatized organic tissues. *In*: H. von Eynatten, J. Reitner, and G. Wörner (eds.), *GV Annual Meeting 2009, Earth Control on Planetary Life and Environment, October 5–7, 2009, Göttingen, Germany*. Abstracts, 33. Reihe der Universitätsdrucke im Universitätsverlag Göttingen, Göttingen.

Forchielli, A., Steiner, M., Hu, S.X., and Keupp, H. 2012. Taphonomy of Cambrian (Stage 3/ 4) sponges from Yunnan (South China). *Bulletin of Geosciences* 87: 133–142.

Forchielli, A., Steiner, M., Kasbohm J., Hu S., Keupp, H. 2013. Taphonomic traits of clay-hosted early Cambrian Burgess Shale-type fossil Lagerstätten in South China. *Palaeogeography, Palaeoclimatology, Palaeoecology* (published online).

Gabbott, S.E., Hou, X.G., Norry, M.J., and Siveter, D.J. 2004. Preservation of Early Cambrian animals of the Chengjiang biota. *Geology* 32: 901–904.

Geidies, H. 1954. Abgeänderte Azan-Methoden. *Mikrokosmos* 42: 239–240.

Han, J., Shu, D., Zhang, Z., Liu, J., Zhang, X., and Yao, Y. 2006. Preliminary notes on soft-bodied fossil concentrations from the Early Cambrian Chengjiang deposits. *Chinese Science Bulletin* 51 (20): 2482–2492.

Hinds, H.R. 1844–45. *The zoology of the voyage of H.M.S. Sulphur, under the command of Capt. Sir Edward Belcher, RN., C.B., F.R.G.S., etc. during 1836–1842*, London, Smith, Elder, and Co., Mollusca, 2 (1): 1–24 (July 1844); 2 (2): 25–48 (October 1844); 2 (3): 49–72 (January 1845).

Holmer, L.E. 1989. Middle Ordovician phosphatic inarticulate brachiopods from Västergötland and Dalarma, Sweden. *Fossil and Strata* 26: 1–172.

Hou, X.G., Aldrige, R.J., Bergström, J., Sieveter, D.J., Sieveter, D.J., and Feng, X.H. 1988. *The Cambrian Fossils of Chengjiang, China. The Flowering of Early Animal Life*. 246 pp. Blackwell Publishing, Oxford.

Hu, S.X. 2005. Taphonomy and Palaeoecology of the Early Cambrian Chengjiang Biota from Eastern Yunnan, China. *Berliner Paläobiologische Abhandlungen* 7: 1–197.

Hu, S.X., Li, Y., Luo, H., Fu, X., You, T., Pang, J., Liu, Q., and Steiner, M. 2008. New record of palaeoscolecids from the Early Cambrian of Yunnan, China. *Acta Geologica Sinica* 82: 244–248.

Hu, S.X., Luo, H., Hou, S., and Erdtmann, B.D. 2007a. Eocrinoid echinoderms from the Lower Cambrian Guanshan Fauna in Wuding, Yunnan, China. *Chinese Science Bulletin* 52: 717–719.

Hu, S.X., Steiner, M., Zhu, M.Y., Erdtmann, B.D., Luo, H.L., Chen, L., and Weber, B. 2007b. Diverse pelagic predators from the Chengjiang Lagerstätte and the establishment of modern-style pelagic ecosystems in the early Cambrian. *Palaeogeography, Palaeoclimatology, Palaeoecology* 254: 307–316.

Hu, S.X., Zhang, Z., Holmer, L.E., and Skovsted, C.B. 2010a. Soft-part preservation in a linguliform brachiopod from the lower Cambrian Wulongqing Formation (Guanshan Fauna) of Yunnan, southern China. *Acta Palaeontologica Polonica* 55: 495–505.

Hu, S.X., Zhu, M.Y., Steiner, M., Luo, H.L., Zhao, F.C., and Liu, Q. 2010b. Biodiversity and taphonomy of the Early Cambrian Guanshan biota, eastern Yunnan. *Science China-Earth Sciences* 53: 1765–1773.

Iijima, M. and Moriwaki, Y. 1990. Orientation of apatite and organic matrix in *Lingula unguis* shell. *Calcified Tissue International* 47: 237–242.

Ivantsov, A.Y., Zhuravlev, A.Y., Leguta, A.V., Krassilov, V.A., Melnikova, L.M., and Ushatinskaya, G.T. 2005. Palaeoecology of the Early Cambrian Sinsk biota from the Siberian Platform. *Palaeogeography, Palaeoclimatology, Palaeoecology* 220: 69–88.

Iwata, K. 1981. Ultrastructure and mineralization of the shell of *Lingula unguis* Linneo (inarticulate, brachiopod). *Journal of the Faculty of Sciences, Hokkaido University (Serie 4)* 20: 35–65.

Iwata, K. 1982 Ultrastructure and calcification of the shells in inarticulate brachiopods. Part 2. Ultrastructure of the shells of *Glottidia* and *Discinisca* [in Japanese]. *Journal of the Geological Society of Japan* 88: 957–966.

James, M.A., Ansell, A.D., Collins, M.J., Curry, G.B., Peck, L.S., and Rhodes, M.C. 1992 Biology of living Brachiopods. *Advances in Marine Biology* 28: 175–387.

Jin, Y., Hou, X., and Wang, H. 1993. Lower Cambrian pediculate lingulids from Yunnan, China. *Journal of Paleontology* 67: 788–798.

Jope, M. 1969. The Protein of Brachiopod Shell III: Comparison with structural protein of soft tissue. *Comparative Biochemistry and Physiology* 30: 209–224.

Jope, M. 1977. Brachiopod shell proteins: their functions and taxonomic significance. *American Zoologist* 17: 133–140.

Kobluk, D.R. and Mapes, R.H. 1989. The fossil record, function, and possible origins of shell color patterns in Paleozoic marine invertebrates. *Palaios* 4: 63–85.

Kowalewski, M. and Flessa, K.W. 1996. Improving with age: the fossil record of lingulide brachiopods and the nature of taphonomic megabiases. *Geology* 24: 977–980.

Kriz, J. and Lukes, P. 1974. Color patterns on Silurian *Platyceras* and Devonian *Merista* from the Barrandian Area, Bohemia, Czechoslovakia. *Journal of Paleontology* 48: 41–48.

Lowenstam, H.A. 1981. Minerals formed by organisms. *Science* 211: 1126–1131.

Luo, H., Fu, X., Hu, S., Li, Y., Chen, L., You, T., and Liu, Q. 2005. New vetulicoliids from the Lower Cambrian Guanshan Fauna, Kunming. *Journal of the Geological Society of China* 79: 1–6.

Luo, H., Fu, X., Hu, S., Li, Y., Chen, L., You, T., and Liu, Q. 2006. New bivalve arthropods from the Lower Cambrian Guanshan Fauna in the Kunming and Wuding areas. *Acta Paleontologica Sinica* 45: 460–472.

Luo, H., Fu, X., Hu, S., Li, Y., Hou, S., You, T., Pang, J., and Liu, Q. 2007. A new arthropod Guangweicaris Luo, Fu et Hu gen. nov. from the Early Cambrian Guanshan Fauna, Kunming, China. *Journal of the Geological Society of China* 81: 1–7.

Luo, H., Hu, S., and Chen, L. 1999. *Early Cambrian Chengjiang Fauna from Kunming Region, China*. 130 pp. Yunnan Science and Technology Press, Kunming.

Luo, H., Li, Y., Hu, S.X., Fu, X., Hou, S., Liu, X., Chen, L., Li, F., Pang, J., and Liu, Q. 2008. *Early Cambrian Malong Fauna and Guanshan Fauna from Eastern Yunnan, China*. 134 pp. Yunnan Science and Technology Press, Kunming.

Mackay, S. and Hewitt, R. 1978 Ultrastructural studies on the brachiopod pedicle. *Lethaia* 11: 331–339.

Manwell, C. 1960. Histological specificity of respiratory pigments-II. Oxygen transfer system involving hemerythrins in sipunculid worms of different ecologies. *Comparative Biochemistry and Physiology* 1: 277–285.

Matthew, G.F. 1902. Notes on Cambrian faunas. *Royal Society of Canada, Transactions* 8: 93–112.

Neary, M.T., Reid, D.G., Mason, M.J., Friscic, T., Duer, M.J., and Cusack, M. 2011. Contrasts between organic participation in apatite biomineralization in brachiopod shell and vertebrate bone identified by nuclear magnetic resonance spectroscopy. *Journal of the Royal Society Interface* 8: 282–288.

Nishizawa, A., Sarashina, I., Tsujimoto, Y., Iijima, M., and Endo, K. 2010. Artificial fertilization, early development and chromosome numbers in the brachiopod *Lingula anatina*. *Special Papers in Palaeontology* 84: 309–316.

Ponomarenko, A.G. 2010. First record of Dinocarida from Russia. *Paleontological Journal* 44: 503–504.

Poulton, S.W., Fralick, P.W., and Canfield, D.E. 2004. The transition to a sulphidic ocean ~1.84 billion years ago. *Nature* 431: 173–177.

Poulton, S.W. and Canfield, D.E. 2005. Development of a sequential extraction procedure for iron: Implications for iron partitioning in continentally derived particulates. *Chemical Geology* 214: 209–221.

Rong, J.Y. 1974. Cambrian brachiopods. In: Nanjing Institute of Geology and Paleontology, Acadamia Sinica (ed.), *Handbook of Palaeontology and Stratigraphy of Southwest China*, 113–114. Science Press, Beijing.

Tazaki, K. 2000. Formation of Banded Iron-Manganese Structures by Natural Microbial Communities. *Clays and Clay Minerals* 48: 511–520.

Steiner, M. 2008. Taphonomy of Early Cambrian phosphatic fossil remains from South China. *Erlanger Geologische Abhandlungen, Sonderband* 6: 64–65.

Steiner, M., Li, G., Hu, S., and Keupp, H. 2010. Soft-tissue preservation in small shelly faunas. *Geological Society of America, Annual Meeting, Denver* 42: 359.

Swinehart, J.H. and Smith, K.H. 1979. Iron and manganese deposition in the periostraca of several bivalve molluscs. *Biological Bulletin* 156: 369–381.

Weber, B., Hu, S.X., Steiner, M., and Zhao, F.C. 2012. A diverse ichnofauna from the Cambrian Stage 4 Wulongqing Formation near Kunming (Yunnan Province, South China). *Bulletin of Geosciences* 87: 71–92.

Williams, A. 1968. Significance of the structure of the brachiopods Periostracum. *Nature* 218: 551–554.

Williams, A. and Cusack, M. 1997. Lingulid shell mediation in clay formation. *Lethaia* 29: 349–360.

Williams, A., Cusack, M., and Buckman, J.O. 1998. Chemico-structural phylogeny of the discinoid brachiopod shell. *Philosophical Transactions of the Royal Society of London, Series B* 353: 2005–2038.

Williams, A., Cusack, M., and Mackay, S. 1994 Collagenous chitinophosphatic shell of the brachiopod *Lingula*. *Transactions of the Royal Society of London, Series B* 346: 223–266.

Williams, A., Lueter, C., and Cusack, M. 2001. The nature of siliceous mosaics forming the first shell of the brachiopod *Discinisca*. *Journal of Structural Biology* 134: 25–34.

Zhang, X. 2007. Phosphatized bradoriids (Arthropoda) from the Cambrian of China. *Palaeontographica Abteilung A* 281: 1–173.

Zhang, X., Hou, X., and Emig, C.C. 2003a. Evidence of lophophora diversity in Early Cambrian Brachiopoda. *Proceeding of the Royal Society of London Series B (Supplement)* 270: 65–68.

Zhang, X., Liu, W., and Zhao, L. 2008a. Cambrian Burgess Shale-type Lagerstätten in South China: Distribution and significance. *Gondwana Research* 14: 255–262.

Zhang, Y., Meng, Q., Jiang, T., Wang, H., Xie, L., and Zhang, R. 2003b. A novel ferritin subunit involved in shell formation from the pearl oyster (*Pinctada fucata*). *Comparative Biochemistry and Physiology Part B: Biochemistry and Molecular Biology* 135: 43–54.

Zhang, Z.F., Han, J., Zhang, X.L., Liu, J.N., and Shu, D.G. 2004a. Soft tissue preservation in the Lower Cambrian linguloid brachiopod from South China. *Acta Palaeontologica Polonica* 49: 259–266.

Zhang, Z.F., Han, J., Zhang, X.L., Liu, J.N., and Shu, D.G. 2007. Note on the gut preserved in the Lower Cambrian Lingulellotreta (Lingulata, Brachiopoda) from South China. *Acta Zoologica (Stockholm)* 88: 65–70.

Zhang, Z.F., Shu, D.G., Han, J., and Liu, J.N. 2004b. New data on the lophophora anatomy of Early Cambrian linguloids from the Chengjiang Lagerstätte, Southwest China. *Carnets de Géologie—Notebooks on Geology, Letter* 4: 1–7.

Zhang, Z.F., Shu, D.G., Han, J., and Liu, J.N. 2005. Morpho-anatomical differences of the Early Cambrian Chengjiang and Recent linguloids and their implications. *Acta Zoologica* 86: 277–288.

Zhang, Z.F., Robson, S.P., Emig, C., and Shu, D. 2008. Early Cambrian radiation of brachiopods: a prespective from South China. *Gondwana Research* 14: 241–254.

Zhao, F., Caron, J.B., Hu, S.X., and Zhu, M.Y. 2009. Quantitative analysis of taphofacies and paleocommunities in the Early Cambrian Chengjiang Lagerstätte. *Palaios* 24: 826–839.

http://dx.doi.org/10.4202/app.2011.0182